

Tectono-stratigraphic evolution of the Late Cretaceous-Eocene of Jordan and implications for the Arabian Plate convergent margin phase

Amir Kalifi^{a,*}, Jihede Haj Messaoud^a, Guillaume Baby^a, Khalil Ibrahim^b, John H. Powell^c, Frans van Buchem^{a,**}

^a KAUST (King Abdullah University of Science and Technology), Thuwal, Saudi Arabia

^b Department of Earth and Environmental Sciences, Prince El Hassan Bin Talal Faculty for Natural Resources and Environment, The Hashemite University, Zarqa, Jordan

^c British Geological Survey (BGS), Nottingham, United Kingdom

ARTICLE INFO

Keywords:

Late Cretaceous
Jordan tectonostratigraphy
Azraq-Hamza Graben
Wadi Sirhan Graben
Santonian event
Arabian Plate

ABSTRACT

The Late Cretaceous-Eocene geodynamic evolution of Jordan is presented, combining, for the first-time, outcrop and subsurface data in this poorly known, yet important part of the Arabian Plate. A new age model developed for outcrop sections, integrating biostratigraphy, C/O and Sr isotopes, together with seismic and well log data significantly improves the timing of the structural events in Jordan and shows their potential relationship to Arabian Plate scale deformation events.

The late Albian-early Turonian displays a gradual north-northwestward thickening trend across Jordan during a phase of tectonic quiescence, whereas in the overlying late Turonian-early Campanian there is ample evidence for extensional/transensional tectonic activity, with an acme during the early Campanian, expressed in the development of the northwest-trending Azraq-Hamza Graben in central-east Jordan. This graben, with an offset of c. 1800 m, extends southeastwards to the Wadi Sirhan Graben in Saudi Arabia and northwestwards to the Levant Basin. The subsequent late Campanian-Eocene succession records reduced tectonic subsidence within the graben during a sag phase and marks a return to regional stability.

The Azraq-Hamza Graben is proven to be time-equivalent to the similarly oriented extensional events in Syria (Euphrates Graben) and Iraq (Sinjar Graben) and is coeval with the compressional structures of the foreland basins in Oman and Iran. This study contributes, to the large-scale tectonic evaluation of the African-Arabian plate deformation and evolution during the Late Cretaceous obduction and subduction phases, which played a critical role in the shaping of the petroleum systems and phosphorite sedimentation of the region.

1. Introduction

The margins of the Arabian Plate became tectonically active during the Late Cretaceous because of a major plate tectonic reorganization initiating the closure of the Neo-Tethys ocean which led to intra-oceanic subduction, and subsequent obduction of ophiolites and continental plate deformation (Ricou, 1994; Vaughan and Scarrow, 2003; Agard et al., 2006; Matthews et al., 2012; Guiraud and Bosworth, 1997; Guiraud et al., 2005). Obduction was widespread from the Mediterranean region to the Himalayas, including the northern and eastern margins of the Arabian Plate (Cyprus to Oman), and occurred over a short time interval (~95-75 Ma) in the Late Cretaceous (Jolivet et al., 2016; Rioux et al., 2016, 2023; Şengör and Stock, 2014). During this brief time

interval, tectonic activity took place over vast regions of the African-Arabian and Eurasian plates, particularly across their convergence zone (Jolivet et al., 2016; Guiraud and Bosworth, 1997).

This tectonic activity induced deformation across the plate, which influenced: (i) the paleogeographical evolution of the Arabian Plate, (ii) the facies distribution and the changing positions of the depocenters, and (iii) the timing and geometry of the elements that make up the regional petroleum systems. In Syria, the Late Cretaceous tectonic deformation played a critical role in the structural setting of petroleum systems in the transensional-driven Euphrates Graben (Brew et al., 1999; Litak et al., 1997, 1998). In Greece, the Late Cretaceous deformation phase is marked by the formation of the Dinaride-Albanide-Hellenide fold-and-thrust belt (e.g. Doutsos et al.,

* Corresponding author.

** Corresponding author.

E-mail addresses: amir.kalifi@kaust.edu.sa (A. Kalifi), frans.vanbuchem@kaust.edu.sa (F. van Buchem).

1993; Papanikolaou, 2009) which played a role in the deposition of source and reservoir rocks, and the timing of structural traps. In the UAE, during this tectonic phase, basement inversion, salt tectonics and detached thrusting was involved in the N- and NE-trending anticlines that form the giant onshore hydrocarbon fields (Johnson et al., 2002, 2005; Abdelmaksoud et al., 2023). Similarly, in Saudi Arabia, this tectonic event induced the formation of the large N-S anticlines that form the traps for the world's largest oil fields (Afifi, 2005; Stewart, 2016).

The tectonic context of the transition from a passive to an active plate margin during the Cretaceous and its effects on the stratigraphy is well documented for the eastern side of the Arabian Plate, through regional compilations (Ricou, 1971, 1974; Glennie et al., 1973; Marlow et al., 2014; Bromhead et al., 2022), and in detailed studies such as of the Oman-UAE mountains (Searle, 1985; Searle et al., 2022; Abdelmaksoud et al., 2022) and the Lurestan Arc of the Iranian Zagros fold-thrust belt (Agard et al., 2005; Farahpour and Hessami, 2012; Homke et al., 2009; Karim et al., 2011; Lalami et al., 2020; Piryaee et al., 2011; Vincent et al., 2015). However, the northern part of the Arabian Plate is less well studied. In the Levant, west of Jordan, compressional deformation was documented during the Santonian (Campanian?) along the Syrian arc deformation belt (Garfunkel, 1978; Gvirtzman et al., 1998), in Egypt (Bosworth et al., 1999) and along the eastern margin of the Levantine and Sinai subplate. In the Negev area, such deformation resulted in folding that influenced accumulation of economically valuable phosphorites and organic-matter rich marls (Gvirtzman et al., 1989). Conversely, in Jordan's northern neighboring countries, major Coniacian-Maastrichtian extensional deformation was reported, namely the NW/SE-trending Euphrates/Anah and Sinjar graben systems in Syria/Iraq, respectively, which created up to 2300 m of accommodation space (Lovelock, 1984; De Ruiter et al., 1995; Litak et al., 1997, 1998; Brew et al., 2001). In Jordan and neighboring Saudi Arabia, a very similar structure developed, the Azraq-Hamza/Wadi Sirhan graben, for which a general Later Cretaceous timing was reported (Andrews, 1992; Abed, 2018; Ye et al., 2023). This structure represents the most significant Late Cretaceous structural deformational event in Jordan (Fig. 1) and was studied during the 1980s and 1990s following oil discoveries in the 'Hamza oilfield' (Core Lab, 1987; Andrews, 1992; Lüning et al., 2014). However, due to lack of age control of the infilling sediments (c. 2000 m of extra-accommodation space created), and poor correlation with outcrop data, the age dating and regional impact of the extensional structures and their fill remained unclear.

Jordan is for, several reasons, a key area to further elucidate the impact of tectonic deformation and stratigraphic impact during the Late Cretaceous to Eocene on the Arabian Plate. The Upper Cretaceous succession (>600m) in Jordan is well exposed in several wadis along a 300 km North-South transect, allowing a high-resolution age model to be established (Messaoud et al., 2025). This Upper Cretaceous succession is characterized by a remarkable lithological variability, displaying, from base to top, a succession of shallow-water carbonate platform sediments, fluvial, marine and deltaic sandstones, chalks, cherts, phosphates and oyster mounds, and finally oil shales. Such a varied succession testifies to the dramatically changing depositional environments, which facilitates stratigraphic correlation in the region. Furthermore, in Jordan, the impact of deformation is limited geographically and temporally, which contrasts to the south-eastern part of the Arabian Plate (e.g. Oman) where the transition from passive to active margins caused a profound structural deformation including obduction and foreland basin formation (Ricou, 1971; Thuizat et al., 1981; Agard et al., 2007; Şengör and Stock, 2014; Jolivet et al., 2016).

This publication addresses the timing, structural character and sedimentary infill of the Upper Cretaceous to Eocene succession in Jordan. First the extensive outcrop/subsurface data set is presented, including the recently established age model (Messaoud et al., 2025). This has provided the time control to establish isopach maps at the scale of Jordan for the main formations. In the discussion the key tectono-stratigraphic findings in Jordan are considered in the broader

context of the geodynamic evolution of the Arabian Plate.

2. Geological setting

The Mesozoic and Cenozoic sediments of Jordan are bounded in the southwest by the Precambrian Basement complex of the Arabian Shield and its Paleozoic sedimentary cover, and in the west by the Dead Sea Transform fault (Fig. 1A). This structure accommodated the relative motion between the African (including Sinai) and Arabian plates (e.g., Quennell, 1958; Garfunkel, 1981; Joffe and Garfunkel, 1987) (Fig. 1B) since the early Miocene (Nuriel et al., 2017), with left-lateral displacements of up to 105 km (Freund et al., 1970; Nairn and Alsharhan, 1997; Bosworth and Burke, 2005; Mart et al., 2005). The eastern flank of the Dead Sea Transform is uplifted, forming prominent escarpments (Fig. 1A). The Mesozoic and Cenozoic succession in this area is relatively undeformed with low-angle dips to the east and was developed within the central Jordan basins, including the Infracambrian Jafr Rift Basin (at depth) in the south and the Late Cretaceous to Early Tertiary Azraq-Sirhan Graben in central eastern Jordan, adjacent to the Saudi Arabian border (Fig. 1A and B). In the northwest, ENE-WSW trending folds and associated faults are part of the Syrian arc (Fig. 1B), which corresponds to an intra-plate fold and thrust belt. The main phase of deformation occurred during the Eocene to Miocene (Chaimov et al., 1992), although a less important earlier phase occurred from the Late Turonian/Coniacian to Santonian/Campanian time (Walley, 1998). The Mesozoic and Paleogene succession is overlain by Neogene to Pleistocene volcanic flows in the Rutbah-Risha region in NE Jordan that formed in response to extensional settings related to the Dead Sea Rift System (Ilani et al., 2001; Shaw et al., 2003).

The Upper Cretaceous to Eocene stratigraphic succession was deposited when Jordan was situated along the southern margin of the Neo-Tethys Ocean (Fig. 1C) (Barrier et al., 2018). During this period, the present-day Ras En Naqb escarpment roughly delineated the paleo-shoreline (Fig. 1A), separating continental environments to the south and east, overlying Palaeozoic strata and the Arabian Shield, from relatively shallow carbonate shelf settings located to the north (Andrews, 1992; Powell and Moh'd, 2011). The continental shelf break was located approximately along the present-day Mediterranean coastline (Alqudah et al., 2023).

The Cretaceous lithostratigraphic succession exposed at outcrop is described in detail by Powell (1989); Powell and Moh'd (2011) and briefly summarized here (Figs. 2 and 3). It starts at the base with the Lower Cretaceous (Albian to Aptian) Kurnub Sandstone Group comprising terrestrial and transitional marine sandstones (Powell et al., 1989). The overlying Cenomanian to Eocene marine succession is subdivided into two groups: the Ajlun Group (early Cenomanian to early Coniacian age), consisting mainly of carbonate platform sediments, and the overlying Belqa Group (late Coniacian to Eocene age), which includes sandstones, chert, phosphates, chalk and organic-rich mudstones (Fig. 2; Powell and Moh'd, 2011). Recently, sedimentological and stratigraphic studies of these groups have been conducted in order to improve the age dating by combining biostratigraphy (including nanofossils, foraminifera and ammonites) and strontium isotope stratigraphy (Messaoud et al. (2025)). This has allowed: (i) improved correlation and age dating of the surface and subsurface lithostratigraphic units, which is the foundation for the construction of the isopach maps presented here, and (ii) placing of the Jordanian tectono-sedimentary events in the broader regional context.

Fig. 2 shows a comparison of the lithostratigraphic nomenclature applied in outcrop and in the subsurface. A similar lithostratigraphic nomenclature has been applied to both for the Ajlun Group and the upper part of the Belqa Group (i.e. Muwaqqar-Chalk-Marl, Umm Rijam and Umm Shallala formations). However, a different lithostratigraphic nomenclature was developed for the lower part of the Belqa Group in the subsurface in the Azraq-Hamza Graben area in the east of the country (Andrews, 1992) (Fig. 2). This difference is caused by the significant

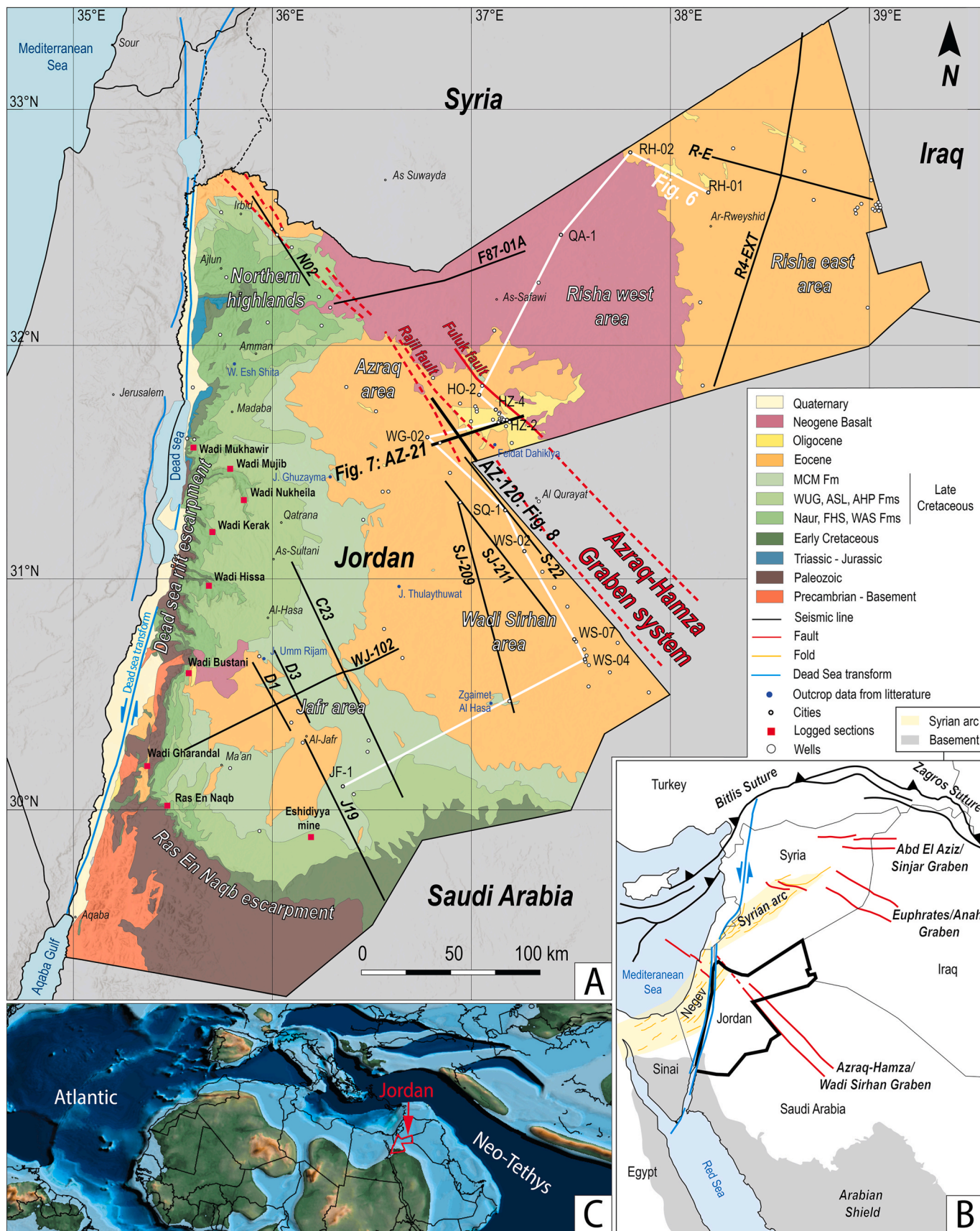
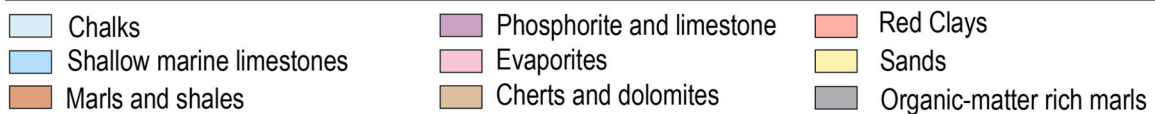


Fig. 1. (A) Geological map of Jordan (compiled from 50k, 100k and 250k geological maps, see Table S1 for references), showing the location of the logged sedimentary sections, the well logs and seismic lines used in this study. The position of the seismic lines shown in Figs. 7 and 8 is indicated, as well as the well log cross-section shown in Fig. 6. For abbreviations used in the legend, see Fig. 2. See Fig. 9A for well names across the entire map; (B) Simplified regional structural map; (C) Paleogeographic map of Jordan and the Neo-Tethys Ocean during the Campanian (80 Ma; Scotese et al., 2025).

Age		Group	West Central Jordan - outcrop Powell and Moh'D. (2011) Messoud et al. (2025)	Stratigraphic units and acronyms This study	Azraq-Hamza Graben - Subsurface Andrews (1992)	
EOCENE		BELQA GROUP	Wadi Shallala Chalk Fm	WSC unit	Wadi Shallala Chalk Fm	
			Umm Rijam Chert-Limestone Fm	UR unit Isopach map, Fig. 9h	Umm Rijam Chert-Limestone Fm	
PALEOCENE			Muwaqqar Chalk Marl Fm <i>K/Pg-ES</i>	MCM unit Isopach map, Fig. 9g	Muwaqqar Chalk- Marl Fm	
			Al-Hisa Phosphorite Fm <i>CM-SB</i>			AHP unit Isopach map, Fig. 9f
LATE CRETACEOUS	Maastrich. Lower		AJLUN GROUP	Amman Silicified Limestone Fm	ASL unit Isopach map, Fig. 9e	Hazim Fm Hamza Fm
	Campanian Upper			Dhiban Chalk Mbr <i>SC-ES</i>	WUG unit Isopach map, Fig. 9d	Upper claystone-limestone unit
				Middle		
	Lower				Alia Sst Mbrs	Lower sandstone unit
				Santonian	Mujib Chalk Mbr	
	Coniacian Late				Khureij Fm <i>TC-ES</i>	Hiatus?
		Middle		Wadi As Sir Limestone Fm	WAS unit Isopach map, Fig. 9c	Wadi As Sir Limestone Fm
	Lower			Walla Lst. Mbr <i>K150-SB</i>	'Lower' Ajlun unit Isopach map, Fig. 9b	'Lower' Ajlun Group
		Upper		Shueib Fm OAE 2		
	Middle			FHS Fms		
Lower		Hummar /Karak Lst Mbr				
	Cenomanian Middle	Fuheis Fm	<i>mC-ES</i>			
Lower		D				
	Lower	Naur Fm C	A			
		B				
Alb.		Kurnub Sandstone Group				



(caption on next page)

Fig. 2. Lithostratigraphy of the Cretaceous to Paleogene strata comparing the Wadi Bustani outcrop section in central Jordan (after Powell & Moh'd, 2011; Messaoud et al., 2025) to the succession in the HZ-2 well located in the Azraq-Hamza-Sirhan graben area c.190 km to the northeast (after Andrews, 1992). The Tafilah Member passes laterally to the Alia Sandstone Member to the southeast, similarly the Hummar Formation passes laterally to the Kerak Formation to the southeast. Fm. = Formation; Mbrs. = members; Lst. = Limestone; OAE= Oceanic anoxic event; Sst. = Sandstone. Abbreviations used in the text are shown. Color code reflects general lithological composition of the lithostratigraphic units. The central column represents the stratigraphic units used throughout the manuscript, and for the construction of the regional isopach maps (Fig. 9), which combine outcrop and subsurface information. Hiatuses age dated by Messaoud et al. (2025) are indicated in italic in the "West Central Jordan – Outcrop" column: mC = Middle Cenomanian; TC = Turonian-Coniacian; CS= Coniacian-Santonian; SC= Santonian-Campanian; CM= Campanian-Maastrichtian; K/Pg = Cretaceous-Paleogene; SB= Sequence boundary; ES=Erosive surface.

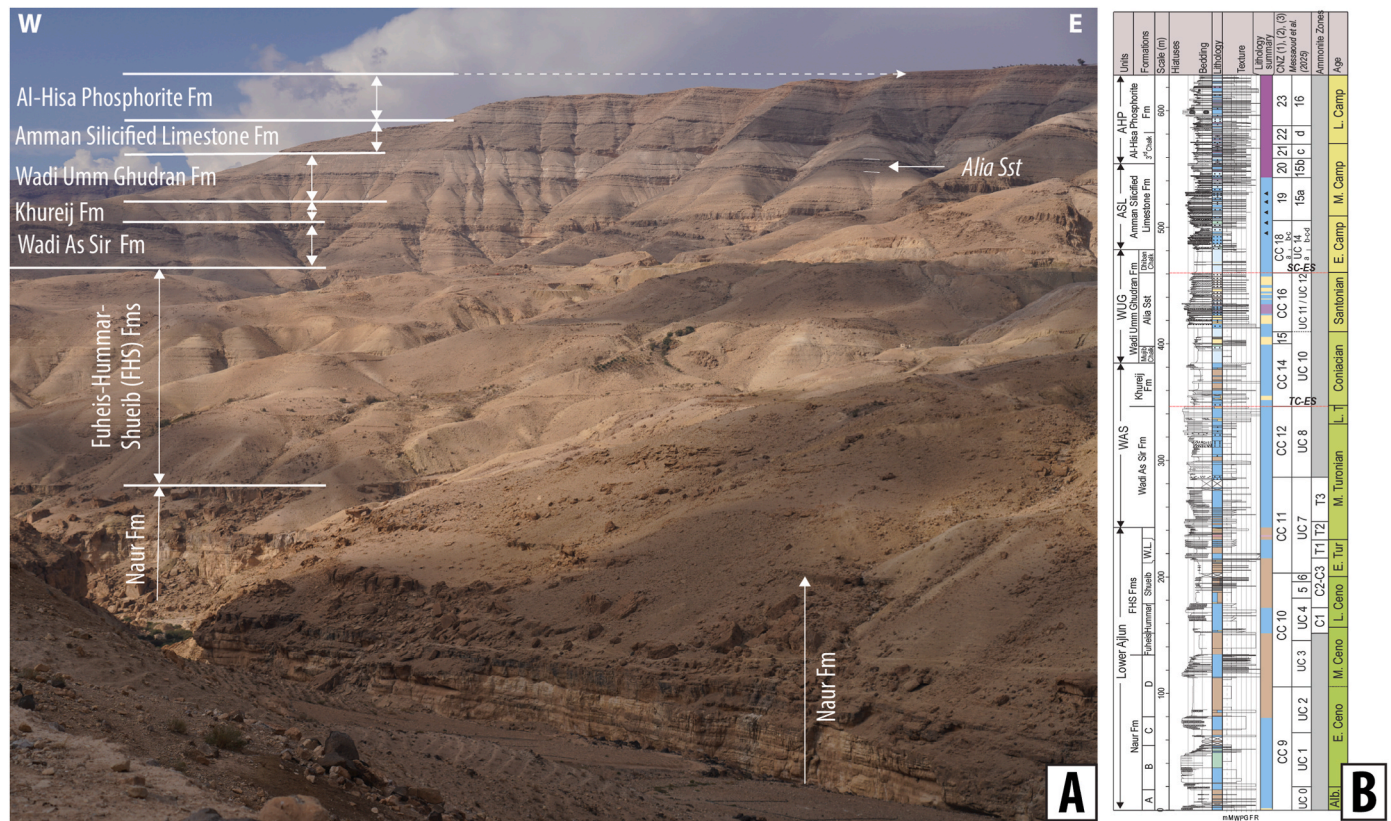


Fig. 3. The Ajlun and Lower Belqa groups in Wadi Mujib. (A) Continuous outcrops of the Upper Cretaceous Ajlun and Belqa groups, displaying the bedding pattern and accessibility. (B) High-resolution age model of the log section (Messaoud et al., 2025). CNZ= Calcareous nannofossils zone; TC = Turonian-Coniacian; SC= Santonian-Campanian; ES=Erosive surface.

variations in thickness and sediment type observed in the graben (Powell, 1989; Andrews, 1992; Abu Saad and Andrews, 1993; Makhoulouf et al., 1996).

The Late Cretaceous NW-SE trending Azraq-Hamza graben system in Central Jordan (Fig. 1A and B) extends into the Sirhan Graben in northeastern Saudi Arabia (Andrews, 1992) and the Galilee Basin towards the Levant (Segev et al., 2018; Wald et al., 2019) (Fig. 1B). The Azraq-Hamza graben system was extensively studied in the 1980s and 1990s following oil discoveries in the 'Hamza oilfield' and reported in unpublished company reports and geological survey (NRA) reports (Core Lab, 1987; Andrews, 1992). Paleozoic thickness variations in the same area (up to twofold) suggest that this structure was inherited and reactivated during subsequent tectonic phases (Andrews, 1992; Abed, 2018).

A synchronous extensive tectonic event occurred in Syria, namely the NW-SE trending Euphrates Graben, which was active from the Coniacian to the Maastrichtian stages (Litak et al., 1997, 1998). Concurrently, compressional deformation along the northern margins of Africa and Sinai, known as the Syrian arc (Bosworth et al., 1999), was also reported. Both are time-equivalent to the intra-oceanic subduction within the central Neotethys, and to the obduction of ophiolite material over the Arabian plate (Jolivet et al., 2016).

3. Materials and methods

3.1. Materials

This paper integrates new and previously published data from both outcrops and the subsurface, a summary of which is provided in the appendix (Table S2).

The outcrop information consists of ten newly logged outcrop sections studied along the Dead Sea rift-facing escarpment (Fig. 1A–Table S2), covering the entire Ajlun and Belqa groups (Fig. 2) (see thickness Table S2). These sections, ranging in thickness from 205 to 670 m, constitute a 350 km long N-S transect from Ras En-Naqb in the south, to Wadi Mukhawir in the north. Three of these sections, Bustani, Mujib and Al Hissa are illustrated in Figs. 3–5. A new age model for these sections, proposed by Messaoud et al. (2025), has improved the stratigraphic resolution to 1–1.5 million years.

Additional outcrop data was sourced from the literature (Powell, 1989; Schulze et al., 2004; Baaske, 2005; Powell and Moh'd, 2011), geological maps and associated bulletins (Ibrahim, 1996; Masri, 2003) and subsurface geological bulletins from the Ministry of Energy and Mineral Resources and the NRA (Andrews, 1992; Makhoulouf et al., 1996).

Fourteen wells were selected from across the country to provide a

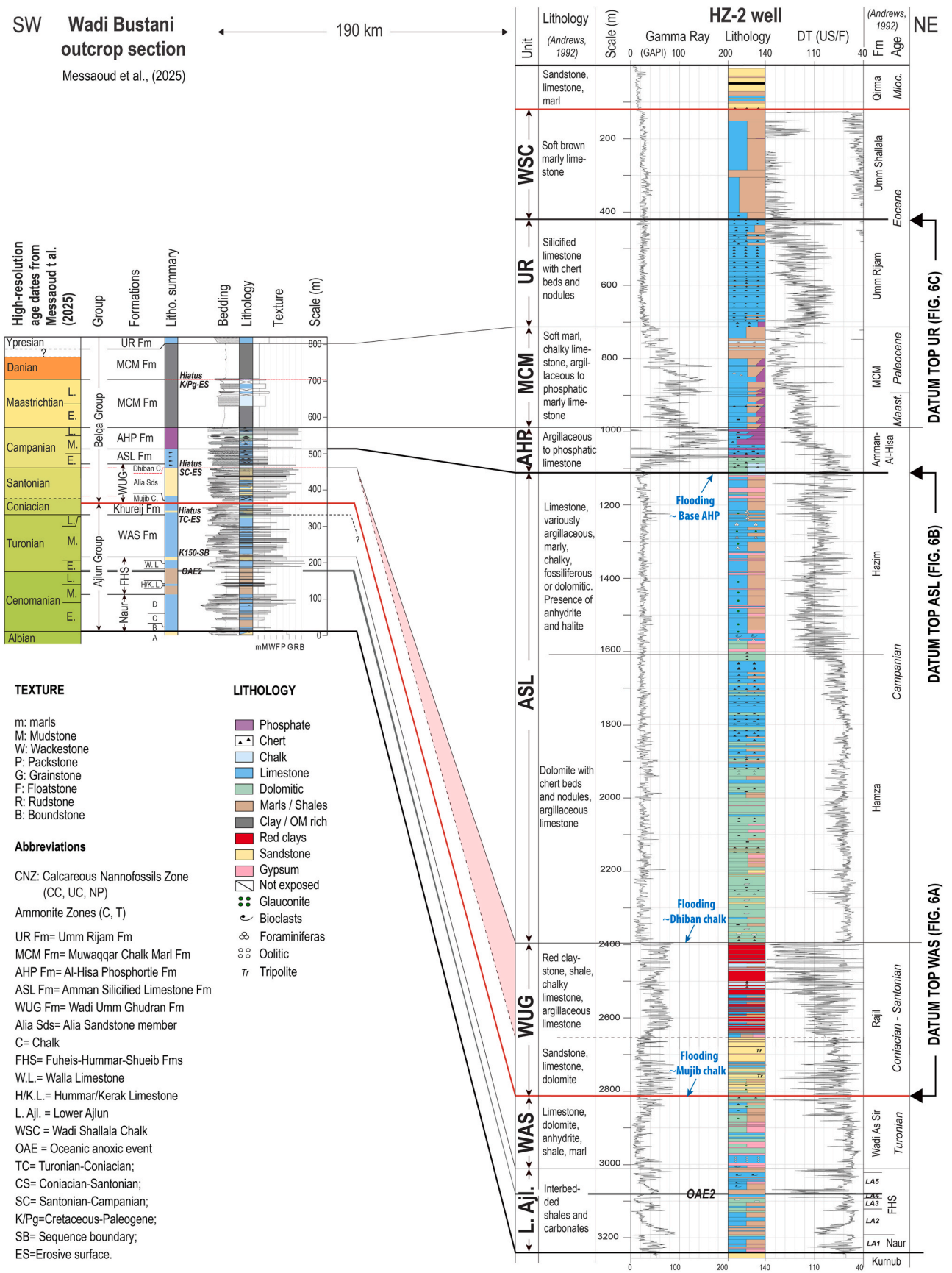


Fig. 4. Correlation of the Wadi Bustani outcrop section to HZ-2 well log. See Fig. 1A for location map.

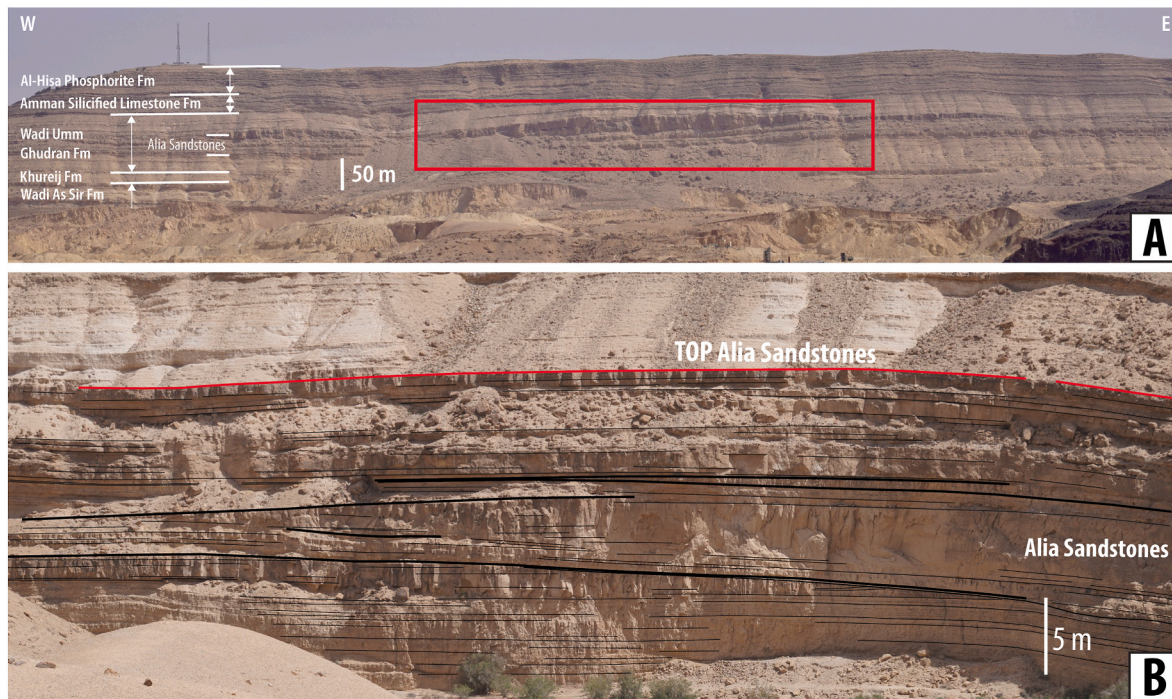


Fig. 5. (A) Overview of the Belqa group in Wadi Hisa, showing prograding delta front sandstone lobes of the Alia Sandstone highlighted in the red square. The upper part of the Ajlun Group and most of the Belqa Group are represented; (B) Nearby tributary valley to Wadi Hisa south from the main wadi: low-angle, large-scale pinch and swell features in a strike view of the prograding sand lobes. Locally some erosion is observed (base middle package on the right).

representative overview of the subsurface stratigraphy; these include gamma-ray, sonic, density and lithological logs derived from cuttings, and are shown in the well log correlations of this paper (Fig. 6). Information from an additional 51 wells (Fig. 1A–Table S2) including lithostratigraphic and thickness data were extracted from subsurface geological bulletins (Andrews, 1992; Abu Saad and Andrews, 1993; Makhlouf et al., 1996) and used to constrain the isopach maps.

Thirteen 2-D seismic reflection profiles were studied to characterize the structural geological context. Two of these are documented in the paper (Figs. 7 and 8). Well-to-seismic ties were established using checkshot data, which were displayed on the intersecting seismic profiles (Fig. 1A).

3.2. Methods

Well-log correlation software was used to compile the dataset (well logs, seismic, seismic to well ties, and outcrop logs). For the stratigraphic subdivision and dating, the subsurface lithostratigraphic framework of Andrews (1992) was used, and the latest age-model established on the outcrop sections (Messaoud et al., 2025). This provided the database for the generation of the isopach maps. Manual corrections have been applied to the isopach maps for outliers induced by software extrapolations. Well-log analysis and correlations have been performed following subsurface stratigraphic principles (e.g. Miall, 2013, 2022; Nichols, 2009; Allen and Allen, 2005). Seismic interpretations have been performed following seismic stratigraphy principles (e.g. Veeken, 2006).

To quantify the vertical displacement (subsidence) within the Azraq-Hamza graben and the other regions in Jordan, the accommodation space was measured using the backstripping method (e.g. Watts and Steckler, 1979) via the BackStrip software by Nestor Cardozo. The backstripping technique allows reconstruction of the subsidence history by sequentially removing the effects of sediment loading and compaction from stratigraphic units to isolate the tectonic subsidence component (Allen and Allen, 1990; Watts, 2001). Total subsidence and tectonic subsidence curves are both proposed. Tectonic subsidence curves isolate crustal movements due to regional tectonics from the sediment loading

and compaction, while total subsidence curves combine both. Formulas, algorithms and parameters such as dry density, porosity coefficient and surface porosity, are taken from Allen and Allen (1990) and Watts (2001). Eustatic sea-level fluctuations values have been taken from published curves (Kominz et al., 2008; Miller et al., 2005).

4. Results

4.1. Lithostratigraphic framework: outcrop to subsurface correlation

The Wadi Bustani section, located in Central Jordan, along with the HZ-2 well in the Hamza oil field within the Azraq area, about 200 km to the NE (Fig. 1A), serve as the key reference sections used to discuss the correlation between the outcropping formations of the Ajlun and Belqa groups and their subsurface equivalents within the Azraq-Hamza Graben (Fig. 4). A comparative table for the lithostratigraphy used in outcrop and in the wells is shown in Fig. 2. The middle column of this figure refers to the units which were used to construct the isopach maps, and are described below. In Fig. 3A, the magnificent outcrops of the Wadi Mujib section are illustrated. The high-resolution chronostratigraphic framework established from nannoplankton and ammonite biozonation for this section is shown in Fig. 3B (Messaoud et al., 2025).

4.1.1. The Ajlun group (Cenomanian – early Coniacian)

4.1.1.1. Lower Ajlun unit – Naur and FHS formations - Cenomanian/early Turonian. The Lower Ajlun unit corresponds to the “Lower Ajlun Group” in the subsurface (Andrews, 1992) and to the Naur and Fuheis-Hummar-Shueib (FHS) formations in outcrop (Fig. 2). The Naur Formation is Early-Mid Cenomanian in age (Messaoud et al., 2025). It comprises an alternation between limestone beds, with low GR values (10–50 API), and shaly intervals with a higher GR response (50–100 API) (Fig. 4). The depositional environment corresponds to shoaling, intertidal to subtidal environments and an inner carbonate platform setting characterized by local rudist reefs and biostromes (Powell and Moh’d, 2011). The overlying FHS formations consist of green mudstones

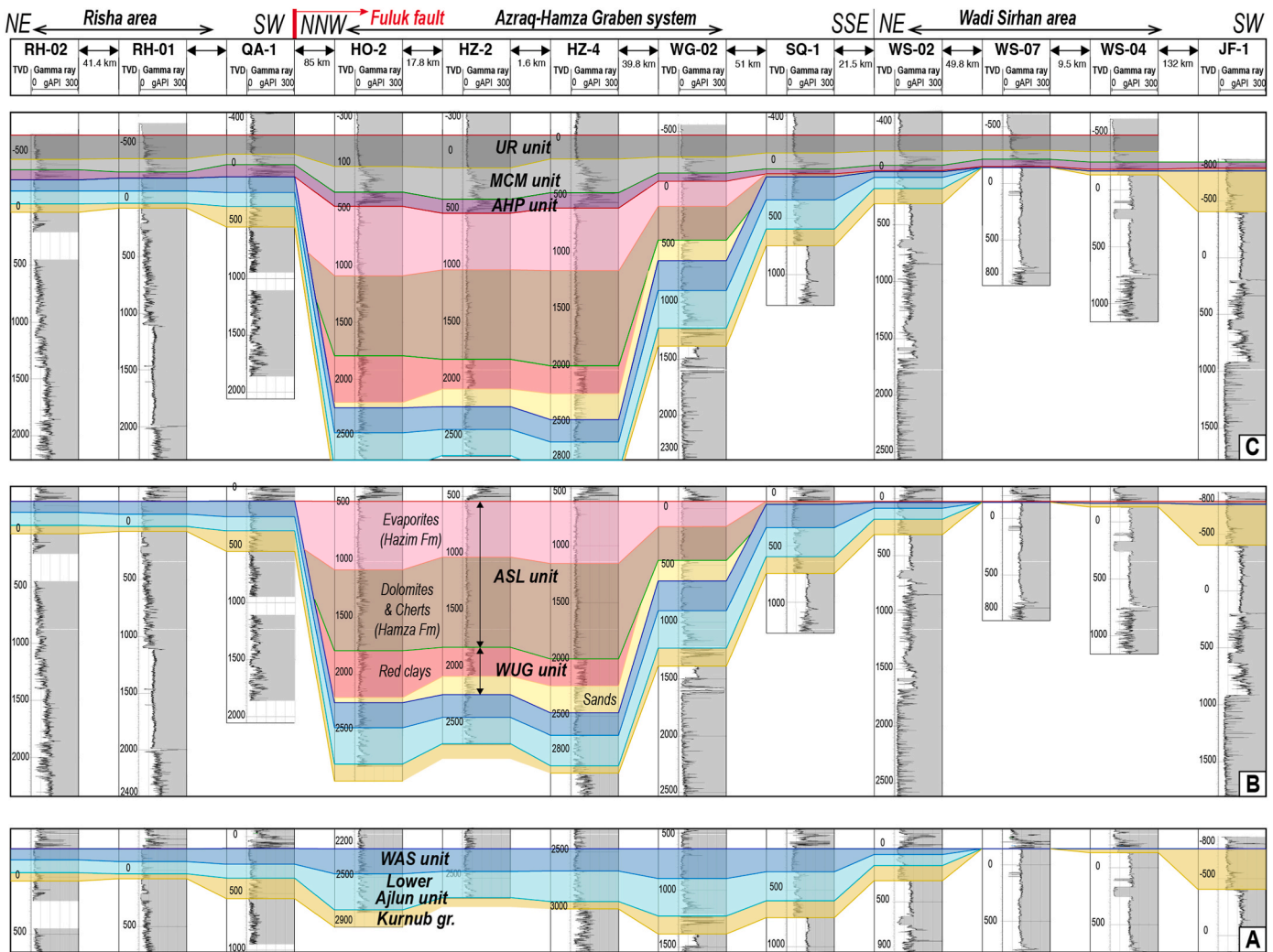


Fig. 6. SW-NE well-log transect across the Azraq-Hamza Graben system. See Fig. 1A for location map. (A) Datum on top of the WAS unit, (B) Datum on top of the ASL unit, (C) Datum on top of the UR unit.

(Fuheis), overlain by a shallow water carbonate unit (Humar, laterally equivalent to the Karak Limestone), which in turn is overlain by green shales and bituminous marls (representing OAE-2), of the Shueib Formation (Powell and Moh'd, 2011). The upper part of this formation contains a thin carbonate member, the Walla Limestone, rich in Early Turonian ammonites, and is overlain by a meter-thick unit of sabkha anhydrites and shoreface sands (Powell and Moh'd, 2011).

In the subsurface, the LA1 unit of Andrews (1992) correlates to the Naur Formation (Fig. 4). The upper LA4 unit is marked by a distinctive bed of dark argillaceous limestone and dark shales with a high organic carbon content (Fig. 4). The Turonian *Bulimnid-Heterohelicid* planktonic biozone (Dilley, 1985; Andrews, 1992) supports the correlation with the Cenomanian-Turonian boundary and the OAE2 event reported in the Wadi Bustani section (Fig. 4; Messaoud et al., 2025). The ooid-rich LA5 cycle (Andrews, 1992) is overlain by a 12 to 25-m-thick sandstone layer with high GR values (60–80 API), which likely corresponds to the sandstones and evaporites of the Shueib Formation at the top of the FHS unit (Fig. 2).

WAS unit - Wadi As Sir and Khureij formations – Mid Turonian to early Coniacian.

The Wadi As Sir Formation is characterized by massive, cliff-forming, well-bedded shallow-marine carbonates at outcrop (Powell, 1989; Messaoud et al., 2025) (Fig. 3). This unit was deposited in a rimmed carbonate shelf and shoaling inner shelf setting (Powell and Moh'd, 2011). The uppermost part of this succession is notable for its abundance

of chert nodules (Fig. 4), a feature observed from Ras En Naqb, in the south, to Wadi Mujib (Fig. 1A). The boundary between the Wadi As Sir Formation and the overlying Khureij Formation represents a depositional hiatus (TC-ES, Fig. 2), where the CC13 nannofossil zone is absent (Messaoud et al., 2025). The early Coniacian Khureij Formation is approximately 30m thick and consists of shallow marine limestones and marls, developed in a rimmed carbonate shelf environment (Powell and Moh'd, 2011).

In the subsurface, the Wadi As Sir Formation consists of shallow-marine carbonates locally interbedded with anhydrite beds in its lower part (Andrews, 1992). This succession exhibits a low GR signature (10–30 API). In its upper part, limestones are interbedded with marls and shales, characterized by a slightly higher GR signature (20–80 API) (Fig. 4). Similar to the outcrop sections, thick beds of chert are present in the uppermost part of the formation in the Azraq and Risha areas (Andrews, 1992; Makhoulouf et al., 1996). At the top of the formation, there is evidence of a possible hiatus, possibly time equivalent to TC-ES hiatus (Fig. 2), in the Wadi Bustani section (Andrews, 1992). The Khureij Formation has not been identified in the subsurface, where the Wadi As Sir Formation is abruptly overlain by the Belqa Group (Fig. 4).

4.1.2. The Belqa group (Coniacian – Eocene)

WUG unit - Wadi Umm Ghudran and Rajil formations – Late Coniacian/Santonian.

The WUG unit consists of the Wadi Umm Ghudran Formation in

outcrop and the Rajil Formation in subsurface (Figs. 2 and 4). The Wadi Umm Ghudran Formation at outcrop is subdivided into three members (Powell, 1989), from the base to the top: (i) the Mujib Chalk member, (ii) a chert-rich siliciclastic unit named Tafilah Member in the north and named Alia Sandstone in the south, and (iii) the Dhiban Chalk member (Fig. 4). The chalk members are interpreted as pelagic ramp (mid-to inner) deposits while the siliciclastic member was deposited in a shallow shoreline depositional environment (Powell and Moh'd, 2011). SC-ES hiatus (Figs. 2, 3B and 4), is marked by a regional hardground, and is evident at the boundary between the chert-dominated Tafilah/Alia Sandstone Members and the overlying Dhiban Chalk Member. Sedimentological details of this hardground are discussed in Powell and Moh'd (2012), and its duration has been estimated at 2.6 Myr (Messaoud et al., 2025). We interpret the Alia marine sandstones as a deltaic system prograding from the south and displaying large-scale, low-angle clinoforms in paleo-dip direction and convex-up geometries interpreted as migrating sand lobes in paleo-strike sections (Fig. 5), which thin and wedge out in a northward direction.

In the subsurface, the equivalent of the WUG Formation corresponds to the Rajil Formation (Andrews, 1992), which is rich in fresh-water *Characeae* (algae) and is divided into two units (Fig. 4).

- A lower sandstone unit with a low GR signature (5–15 API), interbedded at its base with chalky and dolomitic limestone. This alternation is interpreted as the result of fluctuating sea-level in a nearshore deltaic environment (Andrews, 1992). Due to the similar lithofacies associations and stratigraphic position, this unit is likely equivalent in time to the first two members (Mujib Chalk and Tafilah members) of the WUG Formation observed at outcrop (Figs. 2 and 4).
- An upper claystone-limestone unit with a variable, but generally higher, GR response (10–90 API). This unit includes soft, red-brown claystone, grey-green shale, chalky limestone, hard light brown limestone, and sparse beds of sandstone, with an anhydrite layer reported near the base (Andrews, 1992). This succession is interpreted as a transition between terrestrial conditions and shallow-marginal marine deposits (Andrews, 1992). Due to a lack of age dating, correlating this unit is challenging. It might be time-equivalent to either: (i) the SC-ES hiatus (hardground) observed at outcrop at the base of the Dhiban Chalk Member (see above), or (ii) the interval represented solely by the Dhiban Chalk Member of the Wadi Umm Ghudran Fm. In this paper, we propose the first possibility, as the overlying unit in the HZ -2 well exhibits a sharp transition to a chert-rich dolomitic unit of the Hamza Formation, suggesting a rapid transgression more likely to be contemporaneous with the Dhiban Chalk Member (Fig. 3A).

4.1.2.1. ASL unit - Amman Silicified Limestone, Hamza and Hazim formations – Early to Mid. Campanian. In outcrop, the Early to Middle Campanian Amman Silicified Limestone Formation is characterized by abundant chert beds alternating with interbeds of chalk, chalky marls, or limestone rich in a benthic, shallow-water fauna such as gastropods and bivalves (Fig. 4). Locally, oyster build-ups are also present in central Jordan (Masri, 2003). This formation was deposited in a shallow-water, pelagic inner ramp environment (Powell and Moh'd, 2011).

Based on similar lithological characteristics and stratigraphic constraints the Amman Silicified Limestone formation is interpreted as a time equivalent to both the Hamza Dolomite-Chert Formation and the Hazim Formation in the subsurface of Azraq-Hamza Graben (Andrews, 1992; Abu Saad and Andrews, 1993) (Figs. 2 and 4).

- The Hamza Formation consists of dolomite enriched with chert nodules, with sandstone interbeds at the base, and interbeds of argillaceous and chalky limestones at the top (Fig. 4). This formation was deposited in a carbonate shelf setting. The original carbonate

beds have been diagenetically altered to secondary dolomites and cherts (Andrews, 1992). The GR values of this formation typically range from 10 to 40 API.

- The Hazim Formation comprises grey limestone, sometimes dolomitic, marly, chalky, and fossiliferous and contains glauconite. Anhydrite beds are also common, especially towards the top. Up to 30 m thick halite layers are observed in the HZ-4 well (Andrews, 1992) (Fig. 1A). This formation was deposited in restricted marine lagoonal environments (Andrews, 1992). The GR signature of this formation is low and blocky, ranging from 20 to 30 API.

4.1.2.2. AHP unit - Al-Hisa Phosphorite and Amman-Al-Hisa formations – Middle to Late Campanian. In outcrop, the middle to late Campanian Al-Hisa Phosphorite Formation comprises alternating beds of limestone, phosphate and thick oyster mounds (up to 30m high) with a shallow-water fauna including gastropods and bivalves; biogenic chert layers and chalky marls are also present (Fig. 4). This formation was deposited in shallow-water, inner ramp settings (Powell and Moh'd, 2011). The AHP Formation is economically significant and is exploited for both its phosphate content and the pure carbonate of the oyster-mounds (Abed and Sadaqah, 1998; Mustafa et al., 1998; Pufahl et al., 2003; Abed et al., 2007). Moreover, the phosphorite is locally enriched in uranium (Abed and Sadaqah, 2013; Abed et al., 2013).

Previous subsurface studies have grouped the Al-Hisa Phosphorite and Amman Silicified Limestone formations together (Andrews, 1992; Abu Saad and Andrews, 1993). This grouping was primarily adopted in regions where these formations are reduced in thickness and exhibit similar lithologies, making differentiation challenging (e.g., Wadi Sirhan area, Ras En Naqb escarpment, Fig. 1A). However, in central, western, and northern Jordan, particularly in the Azraq area, these formations are well developed and can be distinguished.

4.1.2.3. MCM unit - Muwaqqar-Chalk-Marl Formation – Maastrichtian to Paleocene. In both outcrop and the subsurface, the transition from the Al-Hisa Phosphorite Formation to the Muwaqqar-Chalk-Marl Formation is marked by an abrupt facies change to organic-rich marls, mudstones, and chalk deposited in deep-water pelagic settings across a broad epeiric sea (Powell, 1989; Andrews, 1992; Abu Saad and Andrews, 1993; Powell and Moh'd, 2011) (Fig. 4). This facies change occurs at the Campanian-Maastrichtian boundary (Fig. 4; Messaoud et al., 2025). The organic enrichment occurs in the lower part of the MCM Formation, where the organic matter is immature and of type IIS, with total organic carbon (TOC) ranging from 3 to 30 % (Hakimi et al., 2018; Usman et al., 2025) and was deposited in anoxic and reducing bottom conditions (Andrews, 1992). Consequently, this formation has been considered as a potential unconventional energy resource (Mehdawi and Mustafa, 2007; Hakimi et al., 2016a, 2016b, 2018, b; Abu-Mahfouz et al., 2019, 2020, 2022a, 2022b, 2022c). In the subsurface, the MCM Formation consists of marls with a significant amount of phosphate in the lower half of the unit (Fig. 4). This lithofacies association contrasts with outcrop sections, which are poor in phosphate at this level, except at the very base.

4.1.2.4. UR unit - Umm Rijam Fm. – Early Eocene. The boundary between the Muwaqqar-Chalk-Marl Formation and the Umm Rijam Formation is sharp and is marked by a shift from soft marls and mudstones to porcellanite, hard microcrystalline limestones and chalky limestones with nodules and thin beds of chert (Fig. 4). This formation was deposited in deep-water pelagic conditions, and locally in shallow lagoons (Powell, 1989; Andrews, 1993; Powell and Moh'd, 2011). Throughout Jordan, the transition from Muwaqqar-Chalk-Marl and the Umm Rijam formations occurred consistently at the Paleocene-Eocene boundary (Ali Hussein et al., 2015; Alqudah et al., 2015; Alhejoj et al., 2020; Farouk et al., 2016). The Umm Rijam Formation is rich in both benthic and planktonic foraminifera. Local occurrences of phosphatic limestone are noted, particularly in the Wadi Sirhan and Risha areas

(Andrews, 1992, Fig. 1A). Intervals rich in organic matter are also observed, especially towards the upper part of the unit (Ali Hussein et al., 2014a,b, 2015; Alqudah et al., 2014a,b).

In the subsurface sections, the GR response remains relatively low and consistent at 20–40 API (Andrews, 1992) (Fig. 4). The transition from the Umm Rijam Formation to the overlying Wadi Umm Shallala unit has been dated within the NP15 intra-Lutetian nano-zone (Ali Hussein et al., 2014a,b, 2015; Alqudah et al., 2014a,b; Ahmad et al., 2020).

4.2. Regional well-log transect and seismic

A regional S-N oriented reference well-log transect (Fig. 1A), has been constructed comprising 12 wells with Gamma Ray data, to illustrate the main thickness variations observed in the eastern side of the country, including the Azraq Graben (Fig. 6). The transect has been flattened on three different stratigraphic levels to illustrate the influence of tectonic subsidence on the sedimentation patterns. Subsequently, two seismic lines are presented to show the thickness variations in relation to

the tectonic structures (Figs. 7 and 8). The stratigraphic subdivision used in the following sections are defined in the previous section and summarized in Fig. 2.

4.2.1. The regional well log transect

The first datum, at the top of the WAS unit (~ Early Coniacian), shows a gradual and progressive thinning towards the south of the Lower Ajlun and WAS units (Cenomanian to early Coniacian) (Fig. 6A). These units are absent in the southernmost wells (i.e., WS-07, WS-04, JF-1), suggesting a normal onlap of the platform towards the Arabian Plate hinterland.

The second datum, at the top of the ASL unit (~ Mid Campanian) (Fig. 6B), exhibits a markedly different pattern of thickness for both the WUG and ASL units, particularly within the Azraq-Hamza Graben. Here, sediment thickness reaches up to ~1850m in wells HO-2, HZ-2 and HZ-4, and ~700m in well WG-02. To the north of the graben, no deposits are preserved, while to the south, only a thin layer of the ASL unit, ranging from 10 to 30 m, is present.

The third datum, at the top the UR unit (~intra-Lutetian) (Fig. 6C),

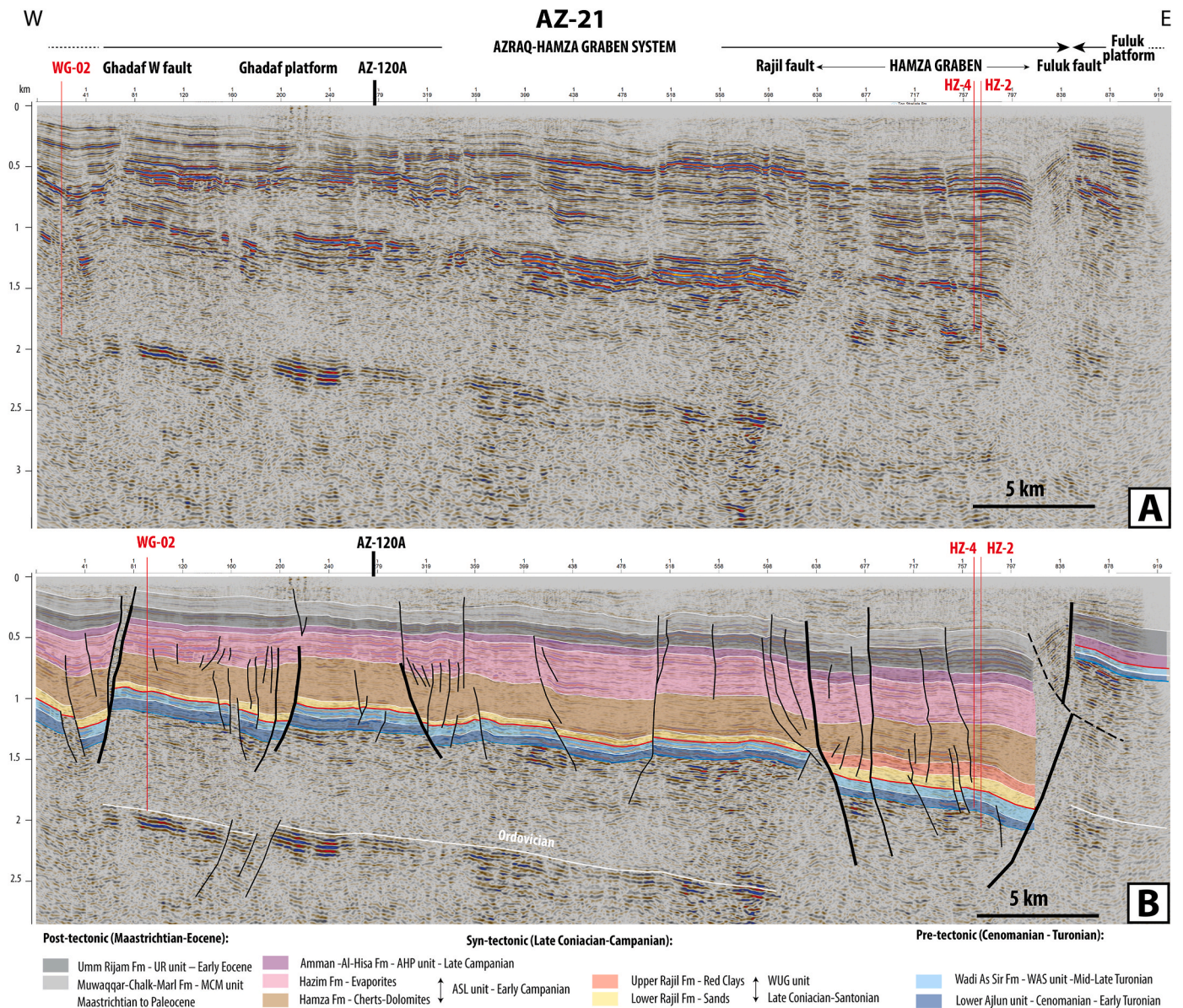


Fig. 7. Seismic Line AZ-21 (see Fig. 1A for location map). (a) uninterpreted line, (b) interpreted line, see text for explanation. Blue line = Base of Ajlun group; Red line = Base of Belqa group. Well positions are shown in red, tied in by cross-shots where they are out of section.

shows a resumption of a generally more uniform subsidence across the entire transect of the AHP, MCM and UR units (Late Campanian – Lutetian). Regionally, these units thin southward, decreasing from ~400m to ~300m, suggesting an onlapping trend towards the Arabian Shield hinterland. Locally, the Azraq-Hamza Graben exhibits a

thickening of the strata, with up to ~600m of sediment preserved in this area suggesting the persistence, although at a much lower subsidence rate, of extensional tectonic activity in the Azraq-Hamza Graben.

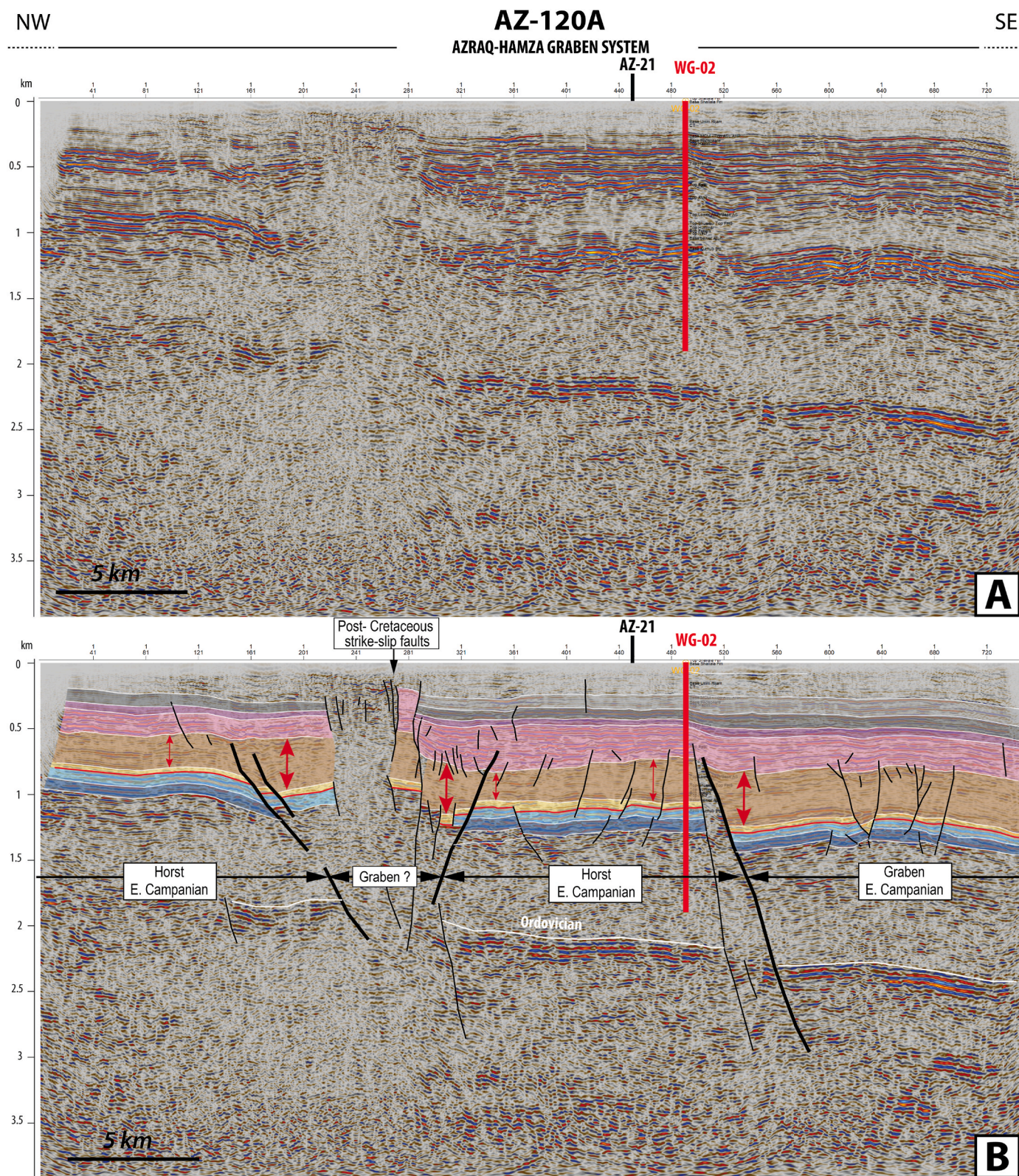


Fig. 8. Seismic Line AZ-120A (see Fig. 1A for location map), (a) uninterpreted line, and (b) interpreted line, see text for explanation. See Fig. 7 for the legend. Red arrows highlight the significant thickness variations. Red line = Base of Belqa Group. The projected WG-02 well is shown in red, tied in by cross-shots.

4.2.2. Seismic profiles across the Azraq-Hamza Graben

For this study 13 seismic lines have been interpreted (Fig. 1A), of which two are shown here (Figs. 7 and 8) to illustrate the main structural features.

The 46 km-long AZ-21 seismic profile, oriented perpendicular to the NW-SE trending Azraq-Hamza Graben (Fig. 1A), reveals part of the geometry of its eastern margin, bounded by the nearly vertical Fuluk master fault (Figs. 6 and 7). The main syn-tectonic Middle Turonian to Middle Campanian sedimentary units, including the WAS, WUG and ASL units, thicken toward this fault (Fig. 7). These units are locally intersected by smaller faults, such as the Ghadaf West and Rajil faults, which control the horsts and grabens (i.e., Ghadaf Platform and Hamza Graben, respectively). These faults also affect younger strata, suggesting tectonic

reactivation after, or synchronous with, the deposition of the Eocene UR unit.

The AZ-120A seismic line (Fig. 8) crosses the Azraq area from SE to NW and is approximately 37 km-long (Fig. 1A). The line is sub-parallel to the NW-SE trending Azraq-Hamza Graben located in the Azraq area. Two normal faults dipping and downthrowing towards the SE are observed along the AZ-120A line. Such a direction could possibly be orthogonal to the SE-NW trending Hamza Graben, or a splay fault off the Rajil Fault (Fig. 8). Another normal fault is dipping and downthrowing towards the NW. These structures suggest two horst and two graben structures (Fig. 8). Approaching the north-western normal faults, seismic resolution decreases due to a narrow zone affected by vertical faults, most likely corresponding to post-Cretaceous strike-slip faults

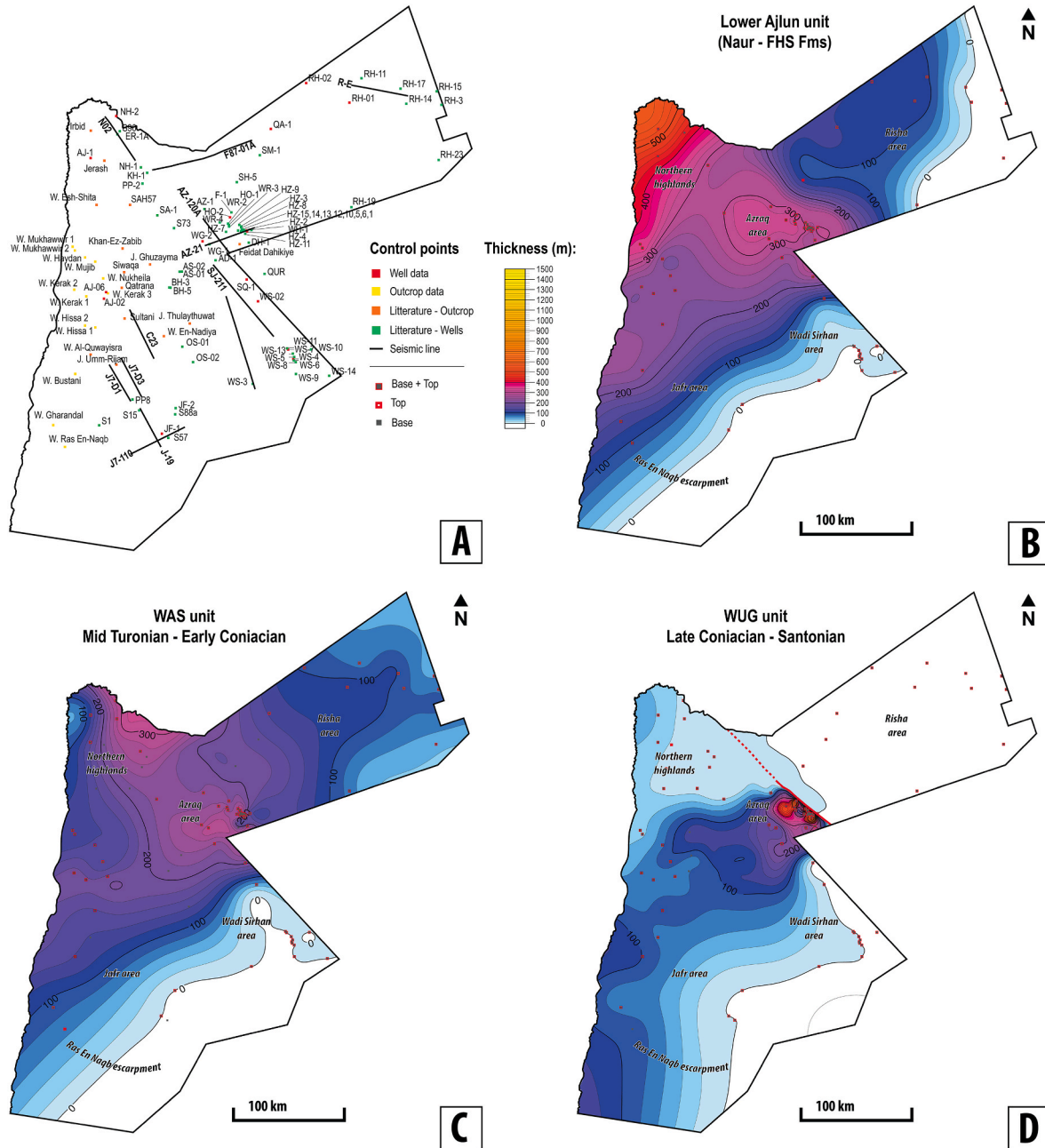


Fig. 9. Isopach maps of the Late Cretaceous to Eocene of Jordan. (A) location map of control points for the isopach maps, see also Table S2; (B) Lower Ajlun unit isopach map (Naur and FHS formations); (C) WAS unit isopach map; (D) WUG unit isopach map. (E) ASL unit isopach map; (F) AHP unit isopach map; (G) MCM unit isopach map; note the initiation of the Jafr Basin possibly controlled by the Karak-Al Hisa fault system, also seen in (H) UR unit isopach map. See Fig. 2 for the definition of the lithostratigraphic units applied for the construction of the isopach maps.

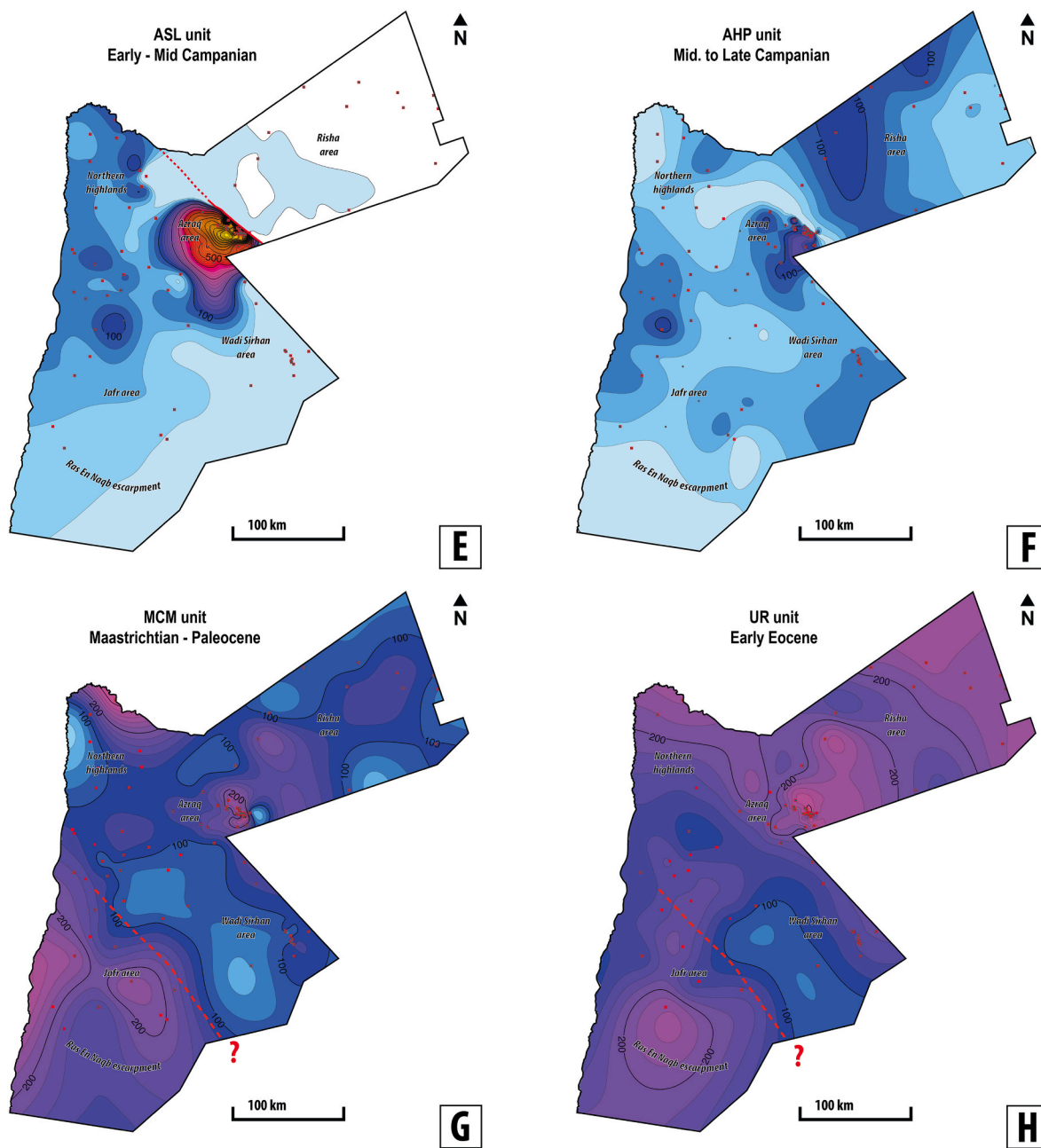


Fig. 9. (continued).

cross-cutting the entire succession (Fig. 8). The Kurnub and Ajlun groups thicknesses do not exhibit any thickness variation, while the Belqa Group displays significant thickness variation, especially the WUG and ASL units. The ASL unit exhibits a significant thickness of ~700m in the normal faults hanging walls (e.g., HZ-2 well, Fig. 4), while reduced thicknesses are observed in the footwalls. Additionally, the normal fault does not crosscut the AHP, MCM and UR units, which suggests that the normal faulting activity is syn- WUG and ASL units time and pre- AHP unit time (Fig. 8).

4.3. Isopach maps

For the construction of the isopach maps, the subsurface data (total of 65 wells) have been combined with 10 outcrop sections measured by the authors, together with 12 additional outcrop control points obtained from the literature, making a total of 87 control points for a total surface

area of 89000 km² (Fig. 9A; Table S2). Seven, country-wide isopach maps have been constructed (Fig. 9B to H) using the units as defined in Fig. 2, and documented in the previous sections.

4.3.1. The Ajlun Group isopach maps – Cenomanian to Coniacian

The isopach maps of the Lower Ajlun unit (Fig. 9B) and the WAS unit (Fig. 9C) reveal a similar regional half-bowl-like geometry, with maximum accommodation preserved in central Jordan, where sediment thickness reaches up to 400 m in the Northern Highlands and Azraq regions for both units. Toward the northeast (Risha Area) and southwest (Jafr and Wadi Sirhan areas) both these units progressively thin, suggesting that these regions represented topographic highs, with a paleo-shoreline located to the southwest of Jordan, oriented approximately NE-SW. In that area, the shoreline position is interpreted from the lateral transition to continental to shallow marine sandstones (Masri, 2010; Powell and Moh'd, 2011).

In the western Risha area (QA-1, RH-01, RH-02), the presence of the Lower Ajlun unit has been confirmed (Abu Saad and Andrews, 1993; Makhoulf et al., 1996), while in the eastern Risha area (RH-03 to RH-26) (Fig. 9B), the Lower Ajlun unit is absent, and the overlying WAS unit sits unconformably on the early Cretaceous Kurnub Sandstone Group (Fig. 9c; Abu Saad and Andrews, 1993; Makhoulf et al., 1996). The boundary between the Risha area and the Azraq area is sharply defined, trending SE-NW. Seismic lines highlight that no thickening occurred due to fault movements (Fig. 7). This thickness trend thus suggests that the Risha area was a paleohigh, which was subsequently fully submerged by WAS unit time indicating increased accommodation, likely linked to a global sea level rise during the Turonian (Miller et al., 2005; Kominz et al., 2008).

In northwest Jordan, the WAS unit is unusually thin (~100–150 m) compared to the more subsiding area along the SE-NW trend in the Azraq-Hamza graben, where the formation thickness reaches about 250 m (Fig. 9C). This thickness trend suggests a subtle shift relative to the underlying Lower Ajlun unit, potentially marking the onset of tectonic activity in the graben. Moreover, the WAS unit in the Azraq-Hamza area is notably rich in evaporites, indicating a shallow depositional environment, while to the west, the formation is characterized by shallow-water carbonates. These differences might suggest that the Azraq area was tectonically isolated during deposition.

4.3.2. The WUG unit – Late Coniacian/early Santonian

The WUG unit is present in all the outcrop sections and reaches its maximum thickness (~400 m) within the NW-SE oriented Azraq-Hamza Graben (Fig. 9D), suggesting its thickness here is synchronous with the activation of this structure. The subsurface equivalent of the upper WUG unit, the red clays of the Rajil Fm (Figs. 2 and 4), is exclusively restricted to the east of the Azraq area (i.e. Azraq-Hamza Graben) and is absent to the west of the Azraq area (i.e. Ghadaf Platform) (Fig. 6B). No sediments of this age are preserved in the Risha region or the southwest of Jordan. Elsewhere, preserved thicknesses are minimal (~50–150 m). The siliciclastic sands constituting the lower WUG unit (Alia Sandstone Member) in the south (Fig. 4) thin northwards and are interpreted as prograding deltaic lobes (Fig. 5). A markedly reduced thickness (<50m) and the absence of sand in the Northern Highlands area suggests either lower sedimentation rate due to reduced subsidence or a tectonically-induced high. Reduced thickness is similarly observed in the underlying WAS unit which could suggest that such tectonically-induced highs have been initiated during Mid-Late Turonian. These observations align with the TC-ES hiatus, identified at the top of the WAS unit in the Wadi Bustani section (Messoud et al., 2025; see Fig. 2), indicating a period of non-deposition and/or erosion likely caused by a fall in relative sea level, with extra accommodation space provided in the tectonically active Azraq Graben. The coastline location and orientation were probably similar as in the underlying Lower Ajlun and WAS units, i.e. trending NW-SE, as testified by a lateral passage to marine and fluvial siliciclastics (Masri, 2010) towards the south-southeast (Arabian Shield) (Fig. 9D).

4.3.3. ASL unit - Early Campanian

The thickness trend of the ASL unit (Fig. 9E) closely resembles that of the WUG unit, with up to 1100m of sediment preserved within the Azraq-Hamza Graben. The AZ-21 seismic line (Fig. 7), which only captures the extreme eastern part of the graben system, provides a limited view, whereas the isopach map (Fig. 9E), offers a comprehensive representation of the thickness variation across the entire graben system. The Hazim Fm, the subsurface equivalent of the upper part of the ASL unit in the Azraq-Hamza Graben (Fig. 2), is rich in evaporitic facies and exclusively restricted to the graben area (Figs. 7 and 8). A consistent thickness of the ASL unit across northern and western Jordan indicates a relatively uniform depositional setting and tectonic stability in these regions. The southern region of Jordan was flooded for the first time since the Cenomanian, suggesting a southward marine transgression,

with a coastline likely positioned in present-day Saudi Arabia. The Risha paleohigh remained exposed, consistent with the trend observed in younger formations.

4.3.4. The AHP unit – Late Campanian

The AHP unit isopach map (Fig. 9F) exhibits a relatively modest thickness of 300 m in the Azraq-Hamza Graben, as compared to ~100 m in other areas, which is significantly less than the thicknesses preserved during the deposition of the underlying WUG and ASL units. This is interpreted as a further slowdown of the tectonic subsidence in the Azraq-Hamza Graben. The AHP unit is more or less isopachous (~100m) in central-west Jordan and shows a reduced thickness (<40m) in the Northern Highlands, consistent with the trend observed in the underlying formations. For the first time within the studied interval, Jordan was entirely covered by marine sediments, the coastline being likely positioned farther south in present-day Saudi Arabia. Phosphate deposition in shallow marine environments occurred in the Ras En Naqb area (south), while a N-S belt of oyster mounds and interfingering phosphate deposits was deposited in central-western Jordan, extending from Al-Hisa to Amman. In the Risha area, a local sandy limestone unit was deposited (Andrews, 1992; see section 4.1.2.).

4.3.5. The MCM and UR units – Maastrichtian-Eocene

The thickness variations of the MCM and UR units reveal two principal ~40 km wide SE-NW trending depocenters (Fig. 9G and H): one located in the Azraq area and the northeastern part of the Northern Highlands, where up to ~250–300 m of sediment were deposited for each formation, and another in southwestern Jordan, extending from the Ras En Naqb escarpment to the Al Hisa and Bustani sections, including the Jafr region, with up to 300 m of sediment preserved for this interval. The eastern Risha area also shows signs of differential subsidence during UR times, which was not as pronounced in the MCM unit. These areas of increased accommodation are likely tectonically controlled, potentially associated with the Azraq-Hamza Graben and the Karak-Al Hisa fault system (Powell, 1989). The central part of Jordan displays reduced subsidence along a NW-SE axis (Fig. 9H). These isopach maps contradict previous models on oil shales development in these units, suggesting that local high TOC and sulfur contents accumulated under anoxic or dysaerobic conditions controlled by small graben systems (Andrews, 1992; Ali Hussein et al., 2015; Alqudah et al., 2015).

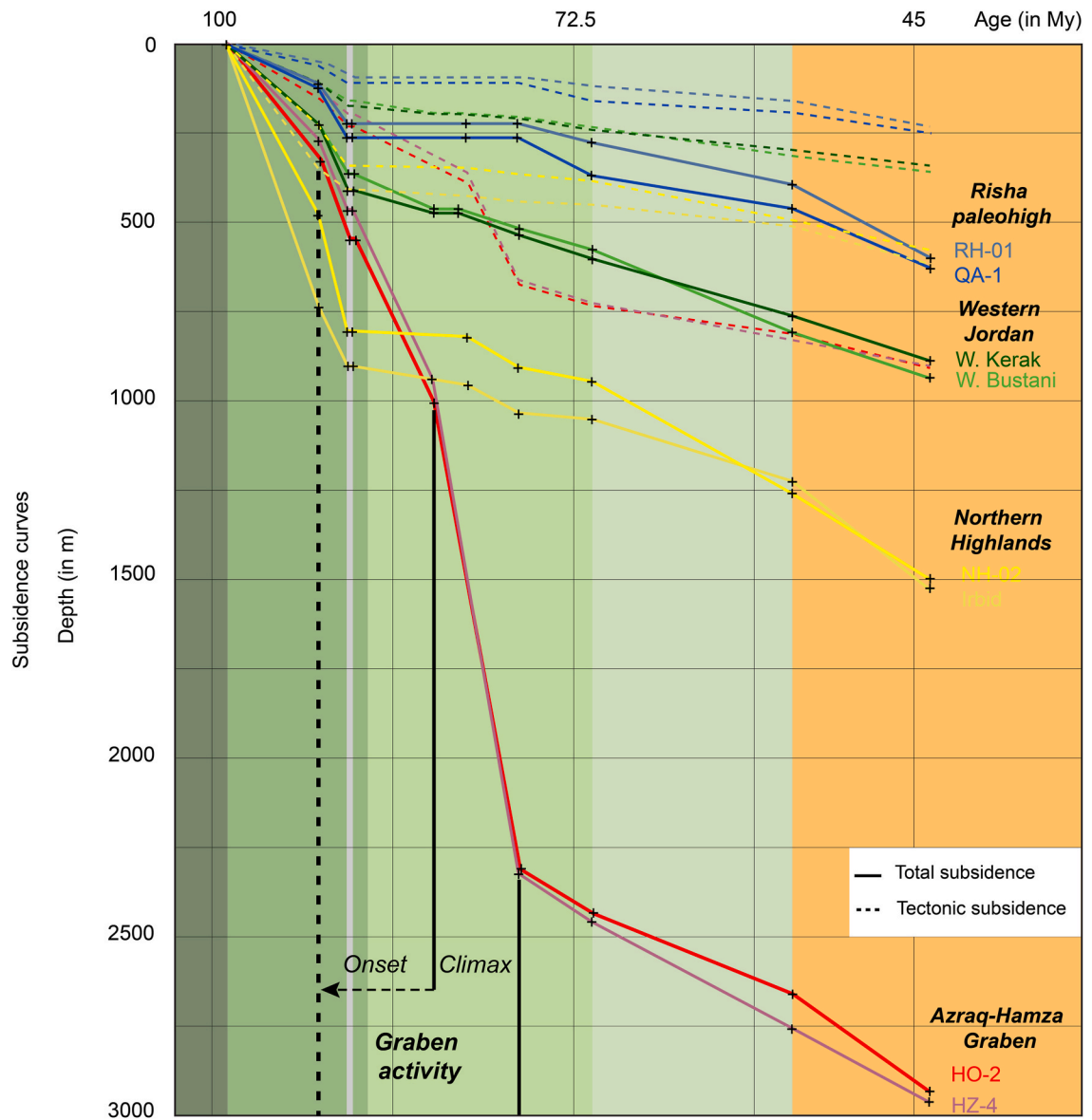
4.4. Subsidence curves

Subsidence curves from the Cenomanian to Mid-Eocene have been constructed for four areas (Fig. 10): the Azraq-Hamza Graben (HO-2, HZ-4 wells), western Jordan (Wadi Bustani outcrop section), the Northern Highlands (Irbid outcrop section and NH-2 well) and the Risha paleohigh (RH-01, QA-1 wells) (Fig. 1A for locations). They reveal distinct trends while highlighting common regional patterns. An acceleration in subsidence is observed during the Turonian in all four regions, indicating a regional-scale tectonic event. Additionally, a cessation of subsidence is noted in the high areas (Risha paleohigh and Northern Highlands) during the active Azraq-Hamza Graben phase, spanning the Turonian to the middle Campanian. During the early Campanian (ASL unit), the subsidence rate of the Azraq-Hamza graben was at a maximum, indicating the most active phase of graben subsidence. Finally, a homogeneous and regional resumption of subsidence is observed from the middle Campanian onward (AHP unit), with nearly identical subsidence rates across the four study areas.

5. Discussion

5.1. Late Cretaceous to Eocene tectonic evolution of Jordan

Four main tectonic phases are recognized of which the principal



Age (in My)	100	95	90	85	80	75	70	65	60	55	50	45	40	35
Chronostratigraphy (GTS)	Early	Late					Paleocene			Eocene				
	Albian	Cenomanian	Turonian	Coniacian	Santonian	Campanian	Maastrichtian	Danian	Selandian	Thanetian	Ypresian	Lutetian	Bartonian	Priabonian
Jordan lithostratigraphy (Messaoud et al., 2025)	Kurnub Group	Lower Ajlun unit	WAS unit	WUG unit	ASL unit	AHP unit	MCM unit			UR unit		WSC unit		
		Ajlun Group			Belqa Group									

Fig. 10. Total subsidence curves and tectonic curves of the Cenomanian-Middle Eocene succession of Jordan, in four different areas. The curves are built using the backstripping method on three outcrop sections and five well logs. See Fig. 1A for the location of the sections. Both tectonic and total subsidence curves have been constructed. The tectonic subsidence curves (dashed lines) isolate crustal movements due to regional tectonics from the sediment loading and compaction, while total subsidence curves (solid lines) combine both.

tectonic features, including faults, folds, and subsidence zones, are illustrated in Fig. 11A, along with their corresponding timing, and thickness variations (Fig. 11B).

- Phase I – Tectonic quiescence (Lower Ajlun unit, Cenomanian to early Turonian) – A bowl-shaped basin configuration (Fig. 10B), with maximum subsidence located in the regions of Azraq and the

Northern Highlands, flanked by inherited topographic highs to the northeast (i.e. Risha Paleohigh) and south (i.e. coastline trending SW-NE, ~ Sirhan-Turayf Paleohigh). Slow regional subsidence is inferred.

- Phase II – Onset of graben (and folding?) development (WAS and WUG units, Mid Turonian to Santonian) – A local rifting event associated with the activation of the Azraq-Hamza Graben (Fig. 11B).

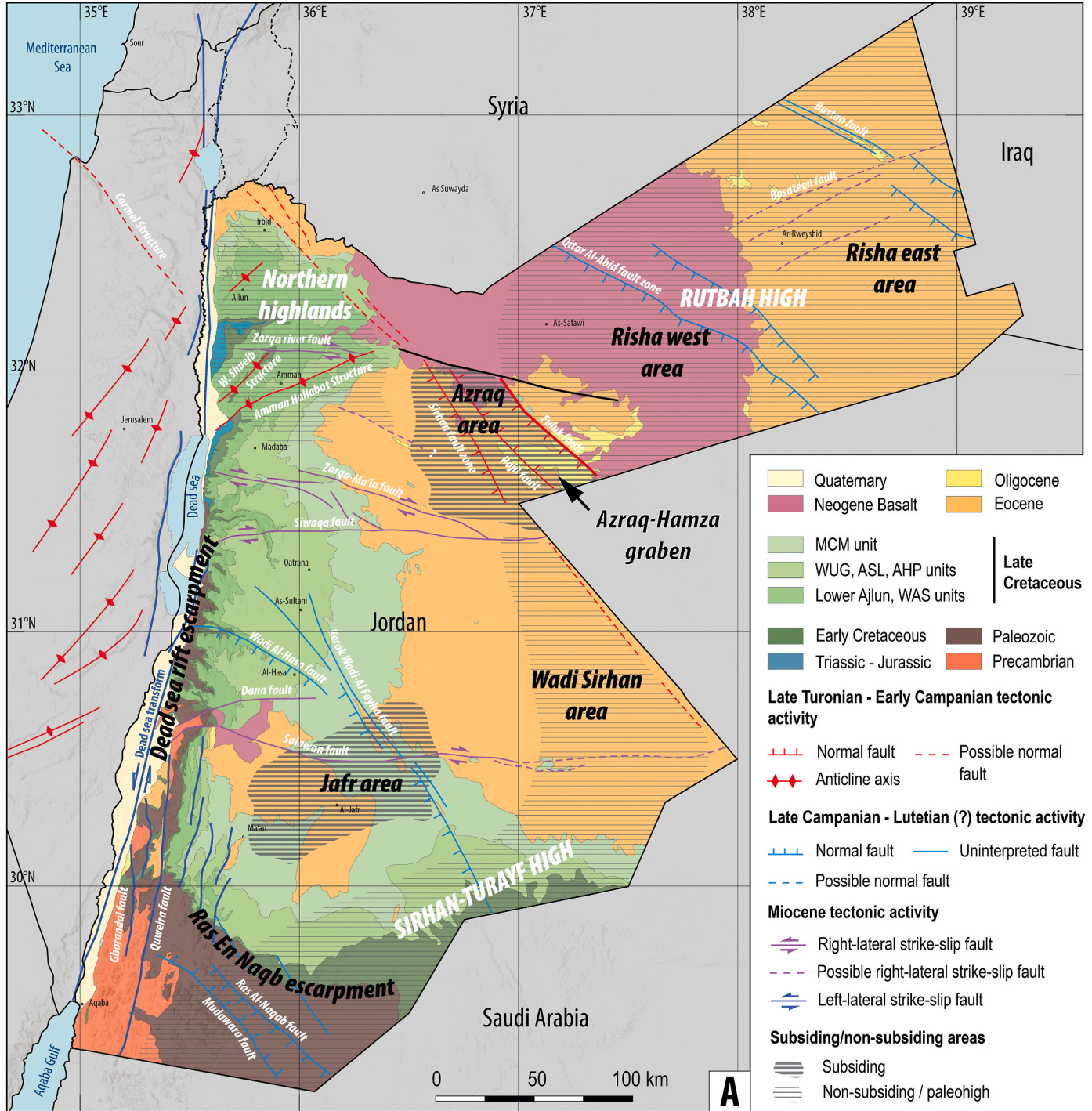


Fig. 11. (A) Structural map of Jordan presenting the general tectonic features and their timing in relation to the geology especially for Late Cretaceous to Eocene time (structures compiled from Barjous (1986), Diabat (2007), Hardy et al. (2010); Powell et al. (2015), and the NRA geological maps at scales of 1:50,000 and 1:250,000). Note that the folds mapped in the Amman area were formed during the Late Cretaceous Syrian Arc Fold system (Mikbel and Zacher, 1986; Al-Zoubi et al., 2006; Al-Awabdeh et al., 2016; Al-Hseinat et al., 2023), and later reactivated as transpressional structures during the Miocene to Recent Dead Sea Transform activity (Al-Awabdeh et al., 2016; Al Hseinat et al., 2023); (B) Tectonostratigraphic summary of Jordan in four phases (P.I to P.IV), showing timing of the tectonic events in relation to the lithostratigraphic units (see Fig. 2 for abbreviations of units), and illustrated with an isopach map and 2 regional cross-section per tectonic phase.

Northern Arabian plate (i.e. Negev, Egypt, Lebanon, [Messoud et al., 2025](#)), and is likely related to the development of a long-lasting (~19 Mys.; Coniacian-Maastrichtian) upwelling system along the Southern Tethys margin ([Almogi-Labin et al., 1993](#); [Meilijson et al., 2014](#); [Alsenz et al., 2013](#), Fig. 1C). This upwelling system is possibly coeval or even partly influenced by a tectonically-driven change in Jordan's carbonate platform morphology, from a rimmed carbonate shelf to a low-gradient homoclinal ramp system ([Powell and Moh'd, 2011](#)).

- Phase III – Graben climax (ASL unit, Early Campanian) – This period marks the end of tectonically-induced highs, associated with folding related to Syrian Arc activity, in the northern highlands (Fig. 11A), and the peak of tectonic activity in the Azraq-Hamza Graben. Lithofacies within the graben during this time were often significantly different from those of the surrounding platform, such as the Hamza and Hazim formations of the ASL unit (Fig. 4B). The total thickness within the graben reached approximately 1400 m, contrasting sharply with the 100–150 m recorded in western Jordan.
- Phase IV – Sag Phase (AHP, MCM, UR units, Late Campanian to Lutetian) – A phase of diffuse extension across the Azraq area subsequent to the earlier extensional phase. The Late Campanian AHP unit signifies a slowdown in tectonic activity, with a more gradual decrease in thickness variations between the graben and surrounding areas (Fig. 9E and F). It is probably associated with the development of NW-SE oriented faults distributed across Jordan (i.e. the Kerak-Wadi Al-Fahya normal fault zone), accompanied by more uniform thermal subsidence at the basin scale (Fig. 11B).

5.2. Structural inheritance

The Late Cretaceous deformation style of the Arabian plate was significantly influenced by inherited tectonic structures ([Barrier et al., 2014](#); [Johnson et al., 2002, 2005](#); [Vergés et al., 2024](#)). In Jordan, [Abed \(2018\)](#), and references therein) showed that the Late Cretaceous Azraq Graben was already active during the Early Cambrian-Ordovician in an extensional regime. This suggests that the Late Cretaceous graben is an inherited structure, potentially linked to the post-orogenic collapse of the East African Orogen and the activation of the Najd Fault System, initiated during the Late Precambrian ([Stern, 1985](#); [Stern and Johnson, 2010](#); [Fritz et al., 2013](#)). The presence of the Risha Paleohigh (i.e. ~crest of the Rutbah High, [Barazangi et al., 1993](#)) during Cenomanian-Early Turonian times (i.e. pre-extension) reinforces the influence of an inherited basement structure (Fig. 9B and C). This structural inheritance may have acted as zones of weakness that were reactivated during the Late Cretaceous (see next section). Additionally, the Sinai and Jordan regions (Fig. 1) experienced regional uplift and alkaline volcanism during the Early Cretaceous ([Gvirtzman et al., 1998](#)), suggesting hotspot activity that may have thermally weakened the lithosphere through heating.

5.3. The Azraq-Hamza Graben Coniacian-Santonian sedimentary infill

Sedimentation within the Azraq-Hamza Graben represents a conundrum, especially the provenance and dispersal of the predominantly siliciclastic deposits in the lowermost Rajil Formation (lower WUG unit) which reaches up to 566 m in HZ 11 well ([Andrews, 1992](#)) but is not represented at outcrop or in the subsurface on the platform. The basal unit ('Lower Sandstone unit') is about 150 m thick and is characterised by white to pale brown, medium-grained, poorly sorted clayey sandstone interbedded with red-brown claystone; cross-bedded, quartz-rich and clayey sandstones intercalated with 'marine' shales are reported from core in HZ-12 ([Andrews, 1992](#)). Sparse interbeds of grey-green mudstone, chalky limestone and dolomitic limestone are also present in the lower part. In the type HZ-2 well (Fig. 4) the sandstone is up to 158 m thick and, regionally, the sandstone is thicker in wells located in the western part of the graben, such as WR-4 ([Andrews, 1992](#)). The overlying 'Upper claystone-limestone' unit, c.280 m thick, is

less sandy and comprises red-brown claystone, grey-green pyritic shale with minor amounts of chalky limestone and pale brown clayey limestone. Age diagnostic fossils are absent in both units, but fresh-water *Characeae* (algae) occasionally associated with ostracods have been described from a few wells ([Andrews, 1992](#)).

The Rajil Formation overlying the early Coniacian Wadi As Sir Formation (limestone) represents the first phase of sedimentation infilling the accommodation space in the rapidly subsiding Azraq-Hamza Graben during late Coniacian time. The presence of chalky limestone, dolomitic limestone and occasional anhydrite suggest a shallow marine environment for this unit lithofacies. However, sandstones and red claystone suggests a terrestrial or coastal plain environment. Furthermore, the presence of thick, cross-bedded sandstones in the west of the graben indicates traction currents.

The question is: what is the provenance of the sand and how was it dispersed into the rapidly subsiding Azraq-Hamza Graben at the same time as chalk-chert-limestone sedimentation on the gently subsiding platform? Siliciclastic sand has not been reported during this interval on the Risha High to the east of the Fuluk Fault, or the platform in central and northwest Jordan, so it is unlikely that it was dispersed from these areas. However, we know that sand was deposited as migrating delta lobes (Alia Sandstone) across the platform/ramp during the Santonian in south and south-central Jordan (e.g. Wadi Hisa, Fig. 5). We hypothesize that the subsiding Azraq-Hamza/Wadi Sirhan Graben formed an elongate, funnel-shaped depression or trough on the sea-floor, which was fed by fluvial siliciclastics in the hinterland to the southeast, passing north-eastwards to clastic coastal plain and sandy shallow marine environments, the latter interdigitating with more typical marine lithofacies during later phases of increased subsidence. Fresh water algae may have been reworked from lagoons in the coastal plain. The 'embayments' shown parallel to the Wadi Sirhan Graben in Fig. 9 D and 9C, 12, may reflect a connection with the southern sandy coastal plain recorded in the Batn El Ghul hinterland area during the late Coniacian and Santonian ([Baaske, 2005](#); [Powell and Moh'd, 2011](#)). The overlying Hamza Chert-Dolomite Formation (up to 840 m thick) marks a virtual shut off of siliciclastic supply from the southeast (only very thin beds of sand are present) and the establishment of shallow marine environments, that kept pace with rapid subsidence within the graben.

5.4. Tectonic evolution of Jordan from a geodynamic perspective at the African-Arabian Plate scale

5.4.1. Late Cretaceous regional tectonics

After a significant plate reorganization (i.e. South Atlantic opening and separation of the South America and African-Arabian plates) and increase of the Africa–Eurasia convergence velocity at ~118 Ma ([Agard et al., 2007](#)), the Late Cretaceous is considered as a period of compression on the African-Arabian Plate with the formation of an intra-oceanic subduction zone in the Neotethys ocean (Trans-Tethyan subduction). This intra-oceanic subduction zone started during the Late Albian (~104 Ma, [Guilmette et al., 2018](#)) and developed during the Late Cenomanian (~96 Ma, Fig. 13A), leading to self-sustained subduction associated with a supra-subduction zone spreading center and the formation of an oceanic lithosphere ([Rioux et al., 2016](#)). The latest was subsequently obducted onto the Arabian plate ([Agard et al., 2007](#); [Jolivet et al., 2016](#); [Ricou, 1971](#); [Şengör and Stock, 2014](#)), with thrusting lasting from Late Cenomanian (~95 Ma) until mid-Campanian (~77 Ma) ([Rioux et al., 2016, 2023](#)) (Fig. 13B). By the late Maastrichtian the foreland basin was formed, and the compressional state ended (Fig. 13C). Whereas the eastern margin of the African-Arabian plate was dominated by a compressional regime from the late Cenomanian till the late Campanian, a wider perspective shows that during that time, extensional structures (NW-SE trending grabens) were a common feature on much of the African-Arabian Plate, such as in Northern Sirte rift, offshore Libya, and the White Nile and Blue Nile rifts in Sudan (Fig. 13B), a pattern that also fits the Azraq-Sirhan Graben, and the other

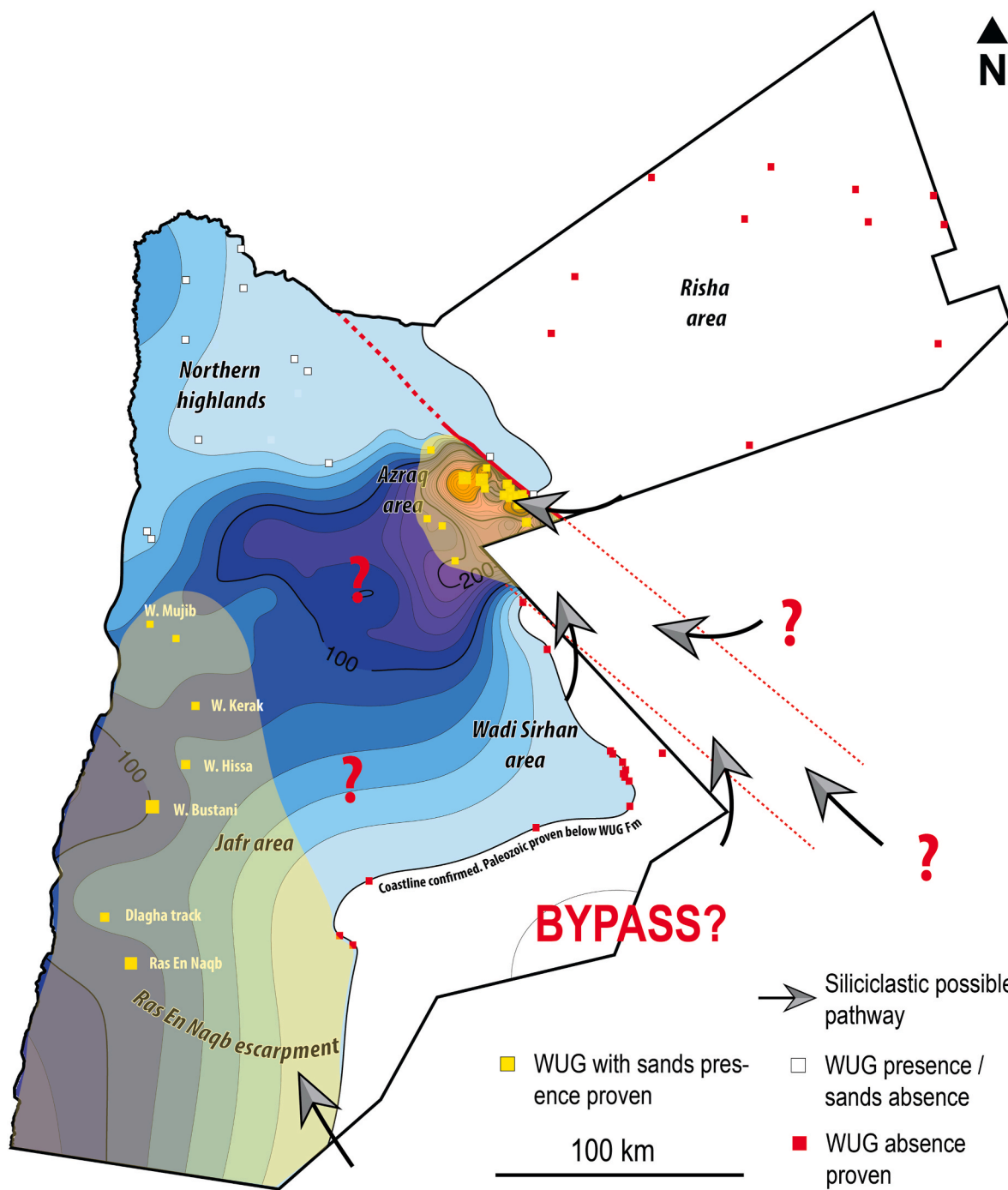


Fig. 12. Extension of Lower WUG unit (Alia sandstone Member in outcrop, and Lower Rajil Fm in subsurface; see Fig. 2) siliciclastic delta of the Late Coniacian-Santonian. See Fig. 4 for the outcropping Alia sandstone member in Wadi Hissa.

Arabian plate grabens, such as the Euphrates Graben (Fig. 14; Litak et al., 1997, 1998) and the Sinjar Trough (Brew et al., 1999). Accompanied by significant Campanian to Maastrichtian sedimentary thickening (2–5 km), and a general absence of syn-rift volcanism, Guiraud and Bosworth (1997) suggested that these rift systems were passive in nature and can therefore be interpreted as resulting from stress relaxation and the transmission of plate boundary forces rather than from active rifting processes.

The other perspective is to consider the Arabian Plate grabens in the context of the Late Cretaceous compressional period and their close location to the convergent eastern Arabian Plate margin (Fig. 15A), and the associated tectonic events comprising, in the North, the so-called

'Santonian Event' (Benkheilil, 1989; Benkheilil et al., 1988; Guiraud and Bosworth, 1997; Bosworth et al., 1999; Guiraud et al., 2005), in the North-East by the emplacement of the 'Syrian Arc' fold belt (Syrian Arc Deformation 1 *sensu* Walley, 1998; Bosworth et al., 1999), in the East by the onset of a foreland basin in the Iran-Iraq fold-and-thrust belt (Farahpour and Hessami, 2012; Lalami et al., 2020; Madanipour et al., 2024; Najafi et al., 2021; Piryaei et al., 2011; Vincent et al., 2015, Fig. 13B), and slightly inboard from this by the formation of N-S oriented folds (Stewart, 2016; Johnson et al., 2002, 2005), the location of some of the world's largest hydrocarbon reservoirs (e.g. Ghawar field; Afifi, 2005). It should be noted that while Fallatah et al. (2025) propose that central Saudi Arabia functioned as a backbulge/forebulge system, this

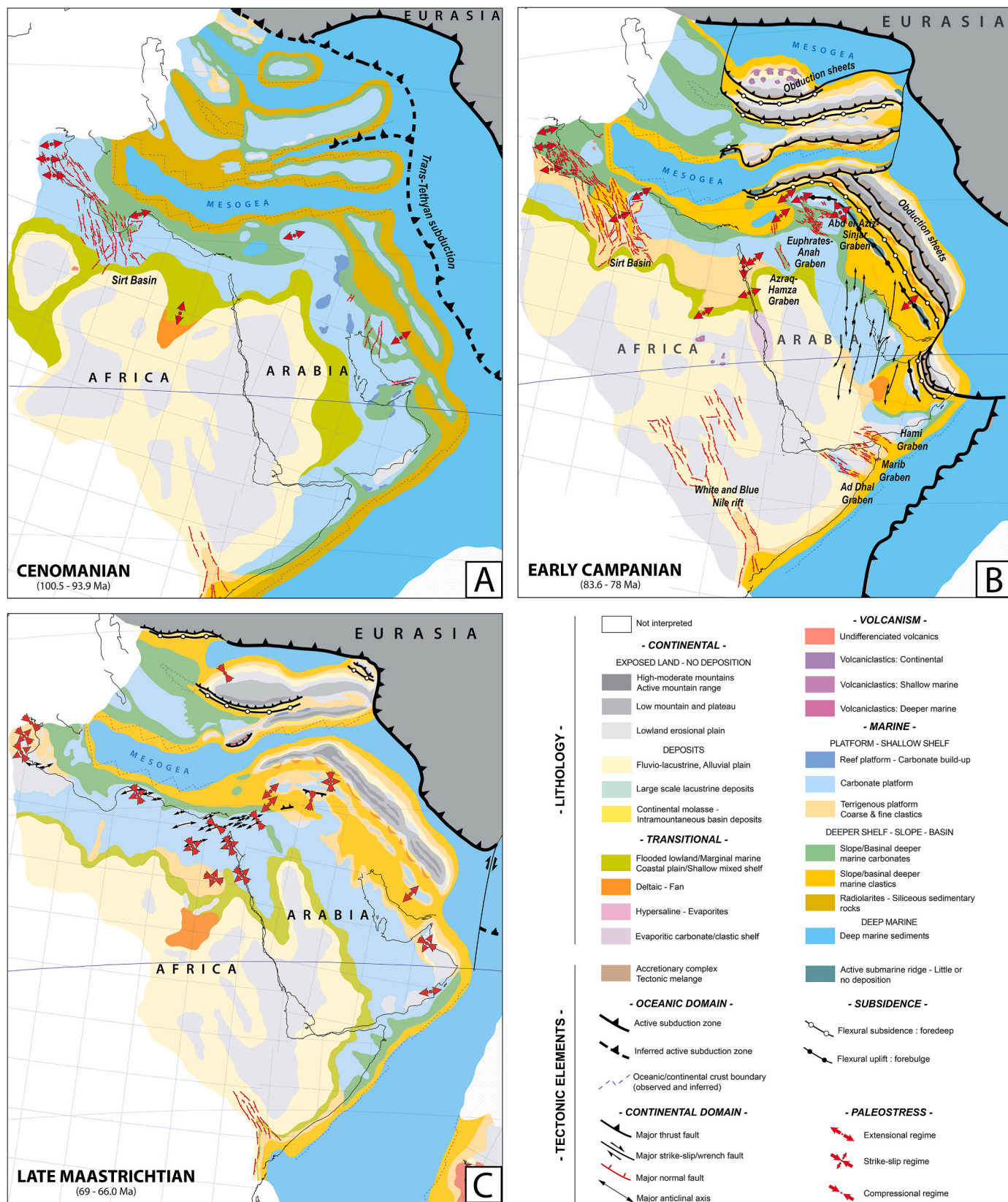


Fig. 13. Late Cretaceous paleotectonic reconstructions of the African-Arabian plate convergence towards Eurasia (modified from Barrier et al., 2018). (A) Cenomanian paleotectonic map (100.5–93.9 Ma), (B) Early Campanian paleotectonic map (83.6–78 Ma), (C) Late Maastrichtian paleotectonic map (69–66 Ma).

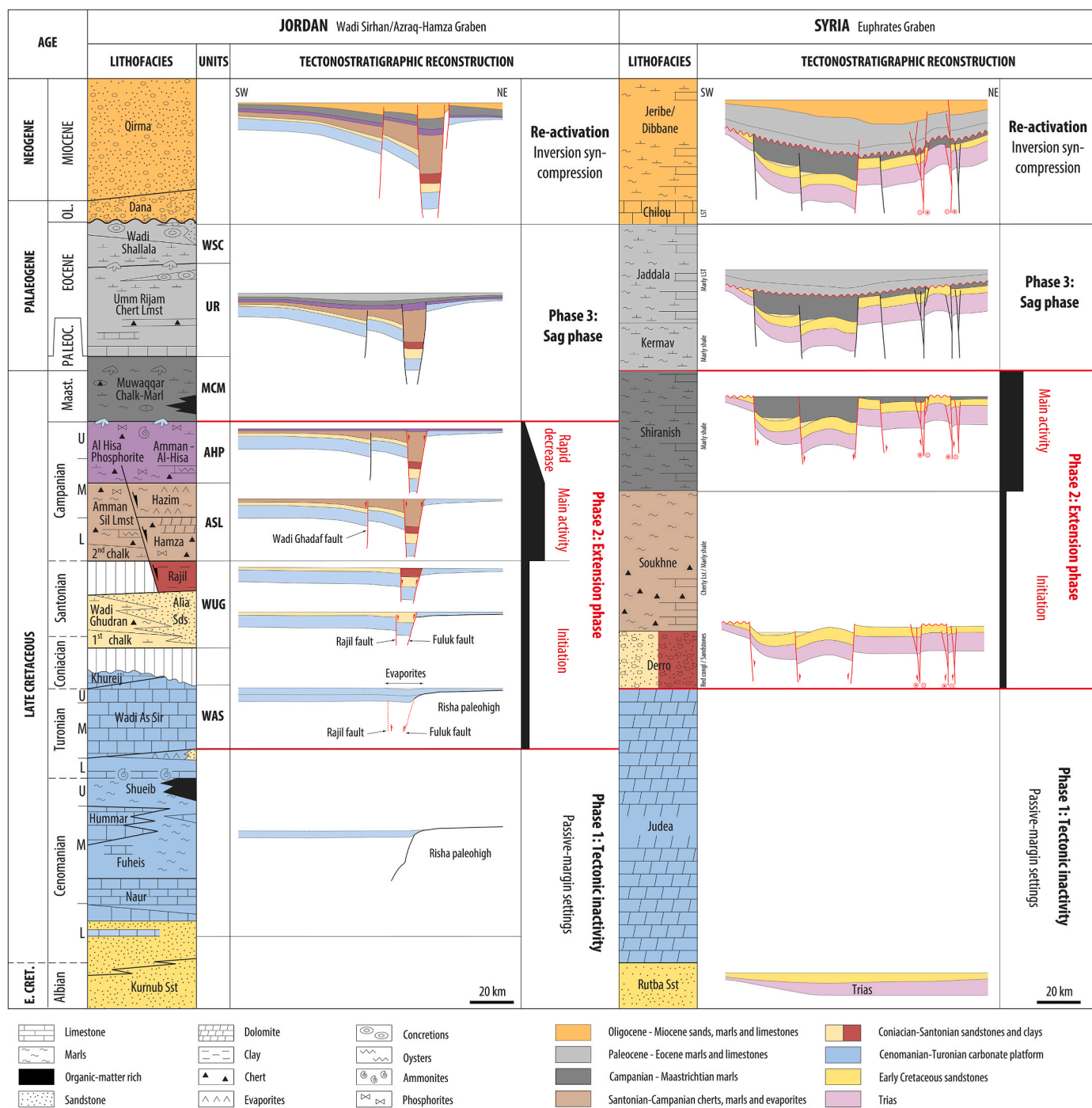


Fig. 14. a) Jordan tectonostratigraphy of the Azraq/Wadi Sirhan graben system (this study), b) Syria tectonostratigraphy of the Euphrates Graben system, modified after Litak et al. (1998).

interpretation contrasts with most existing models, which characterize the region as tectonically quiescent during that time (Figs. 13 and 15a; Barrier et al., 2018; Ziegler, 2001).

The broader plate deformation history described above is pertinent to the tectonic history of Jordan where it is clear that the Azraq-Sirhan Graben subsidence climaxed during the Early Campanian. Our findings suggest that the activation of this graben was partly coeval with the compressive ‘Santonian Event’ (Fig. 11B), and a similar timing was proposed for the opening of the Euphrates Graben. (Figs. 14 and 15C; Litak et al., 1997, 1998). This raises the question: how can compression and extension occur simultaneously? A deeper understanding of this coexistence could enhance our knowledge of the Late Cretaceous

geodynamics of the Arabian Plate, which is essential for a better understanding of how the Late Cretaceous deformation phase propagated across the region and its implications for petroleum systems (i.e. structural features, timing of trap formation, syn-tectonic thickness variations, etc).

Proposing a detailed mechanism for the origin of these intraplate deformations is beyond the scope of this paper. However, we can offer a few hypotheses. It has been demonstrated that a subducting plate can deform internally, depending on plate boundary conditions and the presence of zones of weakness in the lithosphere (e.g., Bellahsen et al., 2003; Capitanio et al., 2009). The Late Cretaceous extensional basins in Arabia were likely inherited from an extensional phase during the Late

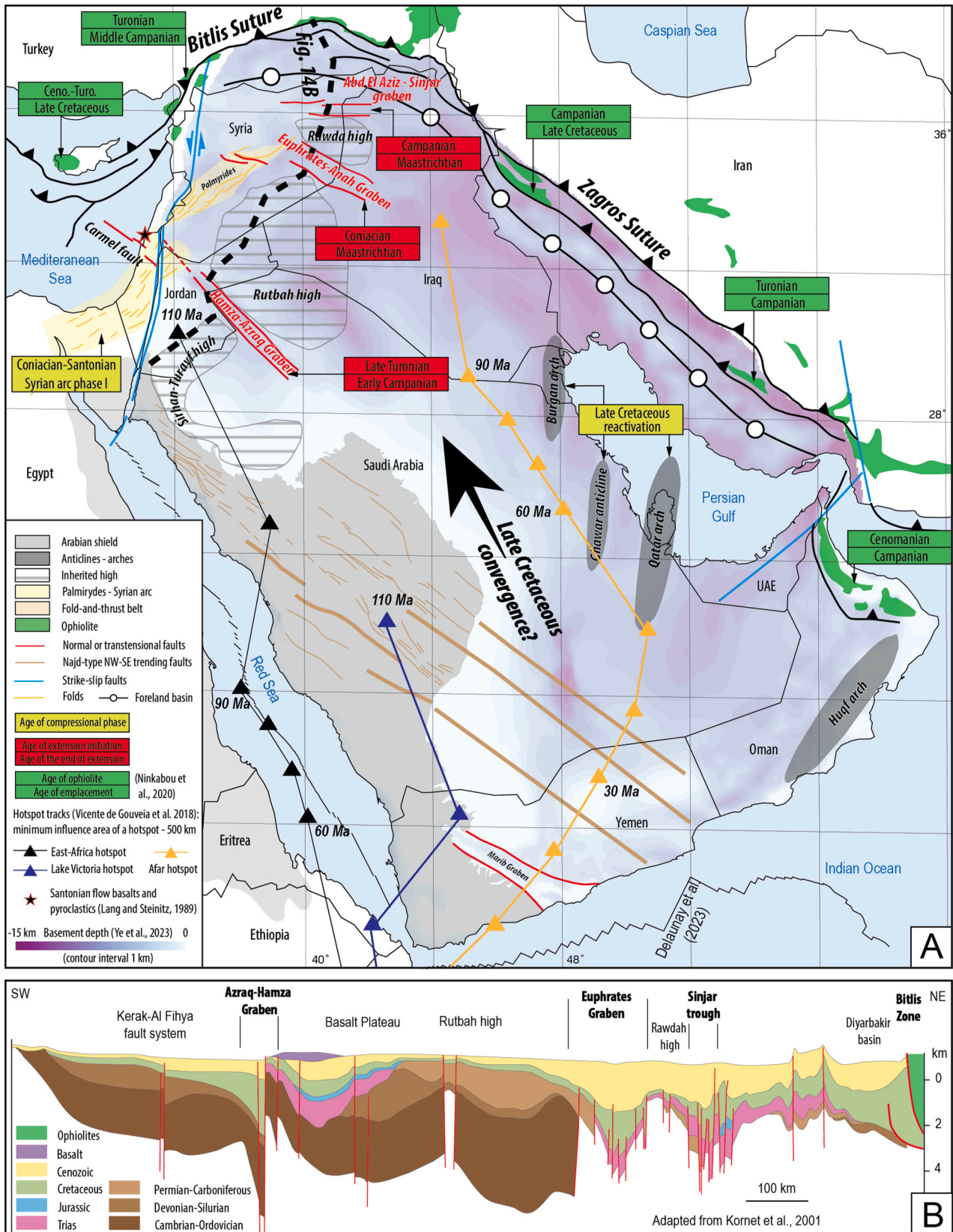


Fig. 15. (A) Middle east structural map displaying the main tectonic elements, especially the Late Cretaceous extensional structures, the Najd-type inherited structures, the Syrian arc and the ophiolites along the Zagros and Bitlis suture. Ages of Ophiolite and emplacement are from Ninkabou et al. (2020). Red Sea spreading axis are from Delaunay et al. (2023). (B) SW-NE cross-section, from Jordan to Turkey. Line of section corresponds to the dotted black line in A. Adapted from Kroonert et al. (2001). (C) Cretaceous tectonostratigraphic chart for the Arabian Plate showing the main structural elements depicted in Fig. 15A.

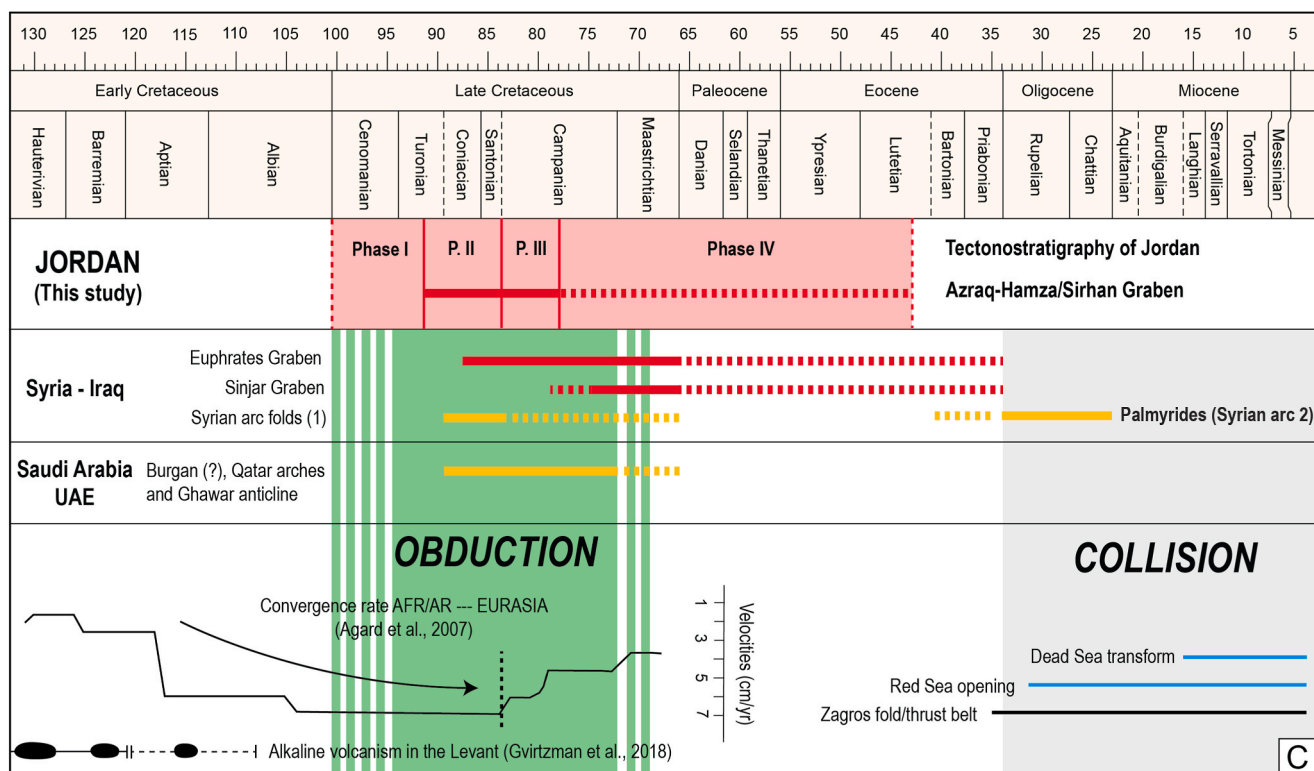


Fig. 15. (continued).

Precambrian (Ediacaran rifting; Powell et al., 2015) and early Cambrian, related to the post-orogenic collapse of the East African Orogen (Fritz et al., 2013). Furthermore, modeling of hotspot tracks in Arabia (Vicente De Gouveia et al., 2018) suggests that intraplate magmatism may have contributed to lithospheric weakening during the Lower Cretaceous, with the traces of the East African and Afar hotspots aligning respectively with the Azraq-Sirhan Graben and the Euphrates Graben (Fig. 15A). Taken together, this hypothesis suggests that these zones of weakness, linked to structural inheritance and/or thermal alteration of the lithosphere, combined with plate boundary conditions, may have locally facilitated intraplate extension within an overall compressive regime.

An alternative scenario is suggested by the hotspot tracks in Arabia (Vicente De Gouveia et al., 2018) which indicate an SSE-NNW plate motion during the Late Cretaceous (Fig. 15A). The sharp shift to a SW-NE motion during the Cenozoic was most likely triggered by the continental collision between Arabia and Eurasia, that induced the Zagros fold-and-thrust belt (McQuarrie, 2002; Mouthereau et al., 2012, Fig. 15A and B). The SSE-NNW motion in the Late Cretaceous would have involved plate convergence in this direction, which is slightly oblique relative to the SE-NW trending Euphrates and Azraq-Hamza graben systems. This suggests that these graben systems, localized along deep-seated basement weakness zones, could have been dominated by transtension, potentially explaining the observed intraplate deformation. Such a hypothesis aligns with detailed structural analyses of the Euphrates graben system, which indicate a transtensional-type structure (Litak et al., 1997, 1998). In this scenario, the large anticlines in Saudi Arabia and the UAE, which host the giant oilfields, would have been formed by transpressional tectonics, developing atop basement structures. This scenario has significant implications for improving our understanding of structural processes and their impact on the Arabian Plate petroleum systems.

5.4.2. The Coniacian – Santonian transition: a regional paleogeographic shift and its impact on sedimentary systems

Late Cretaceous tectonic deformation across the African-Arabian Plate resulted in both local and large-scale sedimentary responses (Ziegler, 2001; Barrier et al., 2018). In Jordan, the local sedimentary responses to the proposed tectonic evolution illustrated in Fig. 11, are: (i) restricted sedimentary systems within the Azraq-Hamza graben system, such as the development and preservation of terrestrial red clays of the WUG unit (Santonian), and the deposition of sabkha evaporites within the uppermost ASL unit (early Campanian) (Fig. 7); (ii) reduced thickness and shallower marine environments in the uplifted Northern Highlands due to the (Late Turonian?)–Coniacian–Santonian compression, led to the absence of siliciclastic sands in the WUG unit (Santonian), and to the deposition of shallow-water chert during the overlying unit ASL unit (early Campanian), as opposed to the deeper water chalks found further south and west on the stable ramp (Powell and Moh'd, 2011); and (iii) northward progradation of a siliciclastic-dominated delta during the late Coniacian–early Santonian (i.e. WUG unit) which might be a local response to uplift of the Arabian Shield hinterland to the south, which resulted in recycling of Paleozoic sandstones in fluvial, passing to coastal plain and delta settings to the northeast.

Additionally, larger scale tectonic-driven sedimentary responses are proposed. In Jordan, the onset of tectonic deformation during middle Turonian is followed in Coniacian time by an abrupt transition from shallow-water carbonate sedimentation on the broad, rimmed shelf of the Ajlun Group, to the highly varied lithologies of the Belqa Group comprising chalks, cherts, phosphorites and organic-rich sediments, deposited on a similarly low-gradient (hemi-pelagic) ramp, but this time with evidence for high marine productivity (Powell and Moh'd, 2011; Messaoud et al., 2025). A similar sharp sedimentary system change was documented in Syria (Barrier et al., 2014), the Negev (Gvirtzman et al., 1989) and Egypt (Kuss, 1992; Kuss and Bachmann, 1996), indicating a marked change in ocean productivity, nutrient supply, biogenic sediment production, and seawater chemistry, most likely due to the development of a long-lasting (~19 Mys.; Coniacian–Maastrichtian)

upwelling system along the Southern Tethys margin (Almogi-Labin et al., 1993; Meilijson et al., 2014; Alsenz et al., 2013, Fig. 1C). Similarly, other Late Cretaceous high-productivity deposits occurred along the northern edges of the African-Arabian Plate, indicating comparable upwelling regimes (Soudry et al., 2006). While climatic and paleoceanographic drivers are commonly proposed to promote such a widespread shift (Meilijson et al., 2018), the synchronicity with the onset of tectonic activity at the scale of the African-Arabian plate (Guiraud and Bosworth, 1997, 2005) would likely add a tectonic component to explain changes in ocean circulation, possibly caused by opening or closure of seaways and/or a change in the ocean floor configuration (Fig. 13).

6. Conclusions

The main conclusions are:

- This study provides a comprehensive synthesis of the Late Cretaceous-Eocene geodynamic evolution of Jordan by integrating both outcrop and subsurface data. The recently published high-resolution age control based on outcrop sections has refined the timing of depositional sequences in the subsurface and associated syn-sedimentary tectonics. A tectono-stratigraphic evolution in four phases is consequently proposed:
 - (i) A tectonically quiet phase, from Cenomanian to early Turonian, consisting of shallow-water carbonate sedimentation on a broad, rimmed shelf, exhibits a regional north-northwest-ward thickening trend and onlap against the Arabian Shield towards the East and South;
 - (ii) The onset of tectonic activity, during the Late Turonian-Santonian period, is characterized by the onset of extensional or transtensional tectonics expressed in the development of the Azraq-Hamza/Wadi Sirhan Graben. This tectonic event is coincident with a dramatic change of the sedimentary system occurring during the Coniacian, comprising a mix of lithologies including, marine sandstones, chalk, and chert on the ramp; in contrast sandstones, red clays and evaporitic deposits were deposited in the graben. The graben initiation phase is roughly synchronous with the development of folds in North Jordan (Late-Coniacian-Santonian ~ a time-equivalent to the 'Santonian event'), impacting thickness and lithofacies distribution;
 - (iii) Active subsidence in the Azraq-Hamza Graben reached a peak during Early Campanian times. The total thickness of syn-tectonic sediments within the graben system reaches 1800 m, comprising predominantly marginal marine sediments.
 - (iv) A post-deformation, sag phase, from Late Campanian to Lutetian, consisting mainly of phosphates, chert and oyster mounds overlain by oil shales and limestone/chert, displays only subtle differential subsidence. The isopach maps contradict previous models of small grabens controlling facies evolution at this time;
- The age constraints of the timing of the Azraq-Hamza Graben also provide a significant improvement of the age control for the timing of the Wadi Sirhan Graben in Saudi Arabia, which was hitherto referred to in the literature as of 'Late Cretaceous' age;
- Correlation and comparison of the Jordanian Azraq Graben with the late Coniacian-Maastrichtian Euphrates/Anah and Campanian/Maastrichtian Sinjar/Abd-el-Aziz grabens (Syria/Iraq) suggests a genetic link of these graben systems to the Late Cretaceous development of a convergent margin and obduction along the eastern and southern margins of the Arabian Plate; we favour the hypothesis that zones of weakness, linked to structural inheritance and/or thermal alteration of the lithosphere, combined with plate boundary conditions, may have locally facilitated intraplate extension or transtension within an overall compressive regime during late Turonian to Maastrichtian times.

- Plate scale considerations of the Late Cretaceous tectonic evolution of the Arabian Plate may have important consequences for the timing of hydrocarbon trap formation.

CRediT authorship contribution statement

Amir Kalifi: Writing – original draft, Visualization, Software, Resources, Methodology, Investigation, Formal analysis, Data curation. **Jihede Haj Messaoud:** Writing – review & editing, Investigation, Formal analysis, Data curation. **Guillaume Baby:** Writing – review & editing, Visualization, Supervision, Software. **Khalil Ibrahim:** Writing – review & editing, Supervision, Project administration, Investigation, Conceptualization. **John H. Powell:** Writing – review & editing, Validation, Supervision, Methodology, Investigation, Conceptualization. **Frans van Buchem:** Writing – review & editing, Visualization, Validation, Supervision, Resources, Project administration, Methodology, Investigation, Funding acquisition, Data curation, Conceptualization.

Declaration of competing interest

The authors declare that they have no known competing financial interests or personal relationships that could have appeared to influence the work reported in this paper.

Acknowledgments

The Jordanian Ministry of Energy and Mineral Resources (MEMR) is gratefully acknowledged for permission to publish the subsurface data. The Hashemite University is acknowledged for the field support and facilitating the administrative formalities in Jordan. This project was financially supported by KAUST (King Abdullah University of Science and Technology) baseline funds of FVB. JHP publishes with the permission of the Director of the British Geological Survey (NERC). Volker Vahrenkamp's and Israa Abu Mafouz's initiative to study the oil shales in Jordan at KAUST was instrumental in getting this study started. Technical discussions with Abdulkader Alafifi and Andika Perbawa are gratefully acknowledged. Field support from Tojo Chirakal, Maria Ardila-Sanchez, Wesam Abu-Leila, and Najeh Ben Chaabane, as well as Petrel support from Yuriy Kaprielov and Mohammad Al-Hamoud, is sincerely acknowledged. Constructive comments by journal editor Tiago Alves and by five referees, three anonymous reviewers, Mike Simmons and Andrea Artoni, helped to considerably improve the clarity of this manuscript. This study was performed by AK in the framework of his post-doctoral research, conducted in KAUST (Thuwal, Saudi Arabia). FVB conceptualized the original research topic of this study, with the support of JHP and KI. Fieldwork was performed by AK, JHM, under the supervision of FVB, KI and JHP. Compilation of outcrop and subsurface data was achieved by AK. Interpretation of subsurface data and construction of isopach maps was conducted by AK, with contributions from FVB. AK wrote the paper, with major contributions from JHM, GB, KI, JHP and FVB.

Appendix A. Supplementary data

Supplementary data to this article can be found online at <https://doi.org/10.1016/j.marpetgeo.2025.107525>.

Data availability

Data is included within the manuscript

References

- Abdelmaksoud, A., Ali, M.Y., Searle, M.P., 2022. Tectono-stratigraphic evolution of the foreland fold-and-thrust belt of the United Arab Emirates. *Tectonics* 41 (9), e2022TC007470.

- Abdelmaksoud, A., Ali, M.Y., Al Suwaidi, A., Koyi, H., 2023. Petroleum system of the fold-and-thrust belt of the United Arab Emirates: new insights based on 1D and 2D basin modeling. *Mar. Petrol. Geol.* 158, 106567.
- Abed, A.M., 2018. Geological evolution of the Azraq basin, eastern Jordan: an overview. *Jordan J. Nat. History* 5 (5), 6–52.
- Abed, A.M., Sadaqah, R., 1998. Role of Upper Cretaceous oyster bioherms in the deposition and accumulation of high-grade phosphorites in central Jordan. *J. Sediment. Res.* 68 (5), 1009–1020.
- Abed, A.M., Sadaqah, R.M., 2013. Enrichment of uranium in the uppermost Al-Hisa Phosphorite Formation, Eshidiyya basin, southern Jordan. *J. Afr. Earth Sci.* 77, 31–40.
- Abed, A.M., Sadaqah, R., Al-Jazi, M., 2007. Sequence stratigraphy and evolution of Eshidiyya phosphorite platform, southern Jordan. *Sediment. Geol.* 198 (3–4), 209–219.
- Abed, A.M., Saffarini, G.A., Sadaqah, R.M., 2013. Spatial distribution of uranium and vanadium in the upper phosphorite member in Eshidiyya basin, southern Jordan. *Arabian J. Geosci.* 7 (1), 253–271.
- Abu Saad, I., Andrews, I.J., 1993. A database of stratigraphic information from deep boreholes in Jordan, *Subsurface Geology Bulletin* 6. Geology Directorate. Subsurface Geology Division, Ministry of Energy and Mineral Resources, NRA, Amman.
- Abu-Mahfouz, I.S., Cartwright, J.A., Idiz, E., Hooker, J.N., Robinson, S., van den Boorn, S., 2019. Genesis and role of bitumen in fracture development during early catagenesis. *Pet. Geosci.* 25 (4), 371–388.
- Abu-Mahfouz, I.S., Cartwright, J., Idiz, E., Hooker, J.N., Robinson, S.A., 2020. Silica diagenesis promotes early primary hydrocarbon migration. *Geology* 48 (5), 483–487.
- Abu-Mahfouz, I.S., Ardila, M., Vahrenkamp, V., 2022a. Geochemical and Petrographic Characteristics of Lithofacies from Upper Cretaceous Organic-Rich Source Rocks, Jordan. *International Petroleum Technology Conference. IPTC. D012S125R003*.
- Abu-Mahfouz, I.S., Gaus, G., Grohmann, S., Klaver, J., Cartwright, J., Idiz, E., Littke, R., Urai, J.L., Patzek, T., Vahrenkamp, V., 2022b. Improved Understanding of Hydrocarbon Expulsion and Associated Fracturing during Successive Stages of Maturation: Insights from the Artificial Maturation of Organic-Rich, Immature to Early Mature Source Rocks. *International Petroleum Technology Conference. IPTC. D031S068R002*.
- Abu-Mahfouz, I.S., Wicaksono, A.N., Idiz, E., Cartwright, J., Santamarina, J.C., Vahrenkamp, V.C., 2022c. Modelling the initiation of bitumen-filled microfractures in immature, organic-rich carbonate mudrocks: the Maastrichtian source rocks of Jordan. *Mar. Petrol. Geol.* 141, 105700.
- Affifi, A.M., 2005. Ghawar: The Anatomy of the World's Largest Oil Field, 20026. *AAPG Search and Discovery*.
- Agard, P., Omrani, J., Jolivet, L., Mouthereau, F., 2005. Convergence history across Zagros (Iran): constraints from collisional and earlier deformation. *Int. J. Earth Sci.* 94, 401–419.
- Agard, P., Monié, P., Gerber, W., Omrani, J., Molinaro, M., Meyer, B., Labrousse, L., Vrielynck, B., Jolivet, L., Yamato, P., 2006. Transient, synobduction exhumation of Zagros blueschists inferred from P-T, deformation, time, and kinematic constraints: implications for Neotethyan wedge dynamics. *J. Geophys. Res. Solid Earth* 111 (B11).
- Agard, P., Jolivet, L., Vrielynck, B., Burov, E., Monie, P., 2007. Plate acceleration: the obduction trigger? *Earth Planet Sci. Lett.* 258 (3–4), 428–441.
- Ahmad, F., Faris, M., Farouk, S., 2020. Calcareous nannofossil biostratigraphy and carbon isotopes from the stratotype section of the middle Eocene Wadi Shallala formation, Northwestern Jordan. *J. Earth Environ. Sci.* 11 (2), 103–112.
- Al Hseinat, M.a., Al-Rawabdeh, A., Al-Zidaneen, M., Ghanem, H., Al-Taj, M., Diabat, A., Jarrar, G., Atallah, M., 2020. New insights for understanding the structural deformation style of the strike-slip regime along the Wadi Shueib and Amman-Hallabat structures in Jordan based on remote sensing data analysis. *Geosciences* 10 (7), 253.
- Al Hseinat, M.a., AlZidaneen, M., Jaradat, R., Al-Rawabdeh, A., Hübscher, C., 2023. Tectono-stratigraphic framework and evolution of the northwestern Arabian plate, Central Jordan. *Tectonophysics* 863, 229993.
- Al-Awabdeh, M., Perez-Pena, J., Azanon, J., Booth-Rea, G., Abed, A., Atallah, M., Galve, J., 2016. Quaternary tectonic activity in NW Jordan: insights for a new model of transpression–transension along the southern Dead Sea Transform Fault. *Tectonophysics* 693, 465–473.
- Al-Zoubi, A.S., Heinrichs, T., Sauter, M., Qabbani, I., 2006. Geological structure of the eastern side of the lower Jordan Valley/Dead Sea rift: reflection seismic evidence. *Mar. Petrol. Geol.* 23 (4), 473–484.
- Alhejoj, I., Farouk, S., Bazeen, Y.S., Ahmad, F., 2020. Depositional sequences and sea-level changes of the upper Maastrichtian-middle Eocene succession in central Jordan: evidence from foraminiferal biostratigraphy and paleoenvironments. *J. Afr. Earth Sci.* 161, 103663.
- Ali Hussein, M., Alqudah, M., Podlaha, O.G., 2014a. Ichnofabrics of Eocene oil shales from central Jordan and their use for paleoenvironmental reconstructions. *GeoArabia* 19 (1), 85–112.
- Ali Hussein, M., Alqudah, M., van den Boorn, S., Kolonic, S., Podlaha, O.G., Mutterlose, J., 2014b. Eocene oil shales from Jordan - their petrography, carbon and oxygen stable isotopes. *GeoArabia* 19 (3), 139–162.
- Ali Hussein, M., Alqudah, M., Blessenohl, M., Podlaha, O.G., Mutterlose, J., 2015. Depositional environment of late cretaceous to Eocene organic-rich marls from Jordan. *GeoArabia* 20 (1), 191–210.
- Allen, P., Allen, J., 1990. *Basin Analysis: Principles and Applications*. Blackwell Scientific Publication, Oxford, London.
- Allen, P., Allen, J., 2005. In: *Basin Analysis: Principles and Applications*, second ed. Blackwell Scientific Publication, Oxford, London.
- Almogi-Labin, A., Bein, A., Sass, E., 1993. Late Cretaceous upwelling system along the Southern Tethys Margin (Israel): interrelationship between productivity, bottom water environments, and organic matter preservation. *Paleoceanography* 8 (5), 671–690.
- Alqudah, M., Ali Hussein, M., Podlaha, O.G., Van den Boorn, S., Kolonic, S., Mutterlose, J., 2014a. Calcareous nannofossil biostratigraphy of Eocene oil shales from central Jordan. *GeoArabia* 19 (1), 117–140.
- Alqudah, M., Ali Hussein, M., van den Boorn, S., Giraldo, V.M., Kolonic, S., Podlaha, O. G., Mutterlose, J., 2014b. Eocene oil shales from Jordan – paleoenvironmental implications from reworked microfossils. *Mar. Petrol. Geol.* 52, 93–106.
- Alqudah, M., Ali Hussein, M., van den Boorn, S., Podlaha, O.G., Mutterlose, J., 2015. Biostratigraphy and depositional setting of Maastrichtian – Eocene oil shales from Jordan. *Mar. Petrol. Geol.* 60, 87–104.
- Alqudah, M., Abu-Jaber, N., Al-Rawabdeh, A., Al-Tamimi, M., 2023. Paleoenvironmental study of the Late Cretaceous–Eocene Tethyan sea associated with phosphorite deposits in Jordan. *Appl. Sci.* 13 (3), 1568.
- Alsenz, H., Regnery, J., Ashckenazi-Polivoda, S., Meilijson, A., Ron-Yankovich, L., Abramovich, S., Illner, P., Almogi-Labin, A., Feinstein, S., Berner, Z., Püttmann, W., 2013. Sea surface temperature record of a Late Cretaceous tropical Southern Tethys upwelling system. *Palaeogeogr. Palaeoclimatol. Palaeoecol.* 392, 350–358.
- Andrews, I.J., 1992. Cretaceous and Paleogene lithostratigraphy in the subsurface of Jordan, subsurface geology bulletin 5. Geol. Dir. Subsurf. Geol. Div. Minist. Energy Mineral Resour. NRA, Amman.
- Baaske, U.P., 2005. *Sequence Stratigraphy, Sedimentology and Provenance of the Upper Cretaceous Siliciclastic Sediments of South Jordan*, PhD Dissertation. University of Stuttgart.
- Barazangi, M., Seber, D., Chaimov, T., Best, J., Litak, R., Al-Saad, D., Sawaf, T., 1993. Tectonic evolution of the northern Arabian plate in western Syria. *Recent Evolution and Seismicity of the Mediterranean Region*, pp. 117–140.
- Barjous, M.O., 1986. The geology of Siwaqa, map sheet No. 3252-IV, Bulletin. Geol. Dir. Geol. Mapp. Div., NRA, Amman 4.
- Barrier, E., Machhour, L., Blaizot, M., 2014. Petroleum Systems of Syria.
- Barrier, E., Vrielynck, B., Brouillet, J., Brunet, M., Angiolini, L., Kaveh, F., 2018. Paleotectonic reconstruction of the Central Tethyan Realm. *Tectono-Sedimentary-Palinspastic Maps from Late Permian to Pliocene. CCGM/CGMW, Paris. Commission for the Geological Map of the World atlas of, 20*.
- Bellahsen, N., Faccenna, C., Funicello, F., Daniel, J., Jolivet, L., 2003. Why did Arabia separate from Africa? Insights from 3-D laboratory experiments. *Earth Planet Sci. Lett.* 216 (3), 365–381.
- Benkheilil, J., 1989. The origin and evolution of the cretaceous Benue trough (Nigeria). *J. Af. Earth Sci. (and the Middle East)* 8 (2–4), 251–282.
- Benkheilil, J., Dainelli, P., Ponsard, J., Popoff, M., Saugy, L., 1988. The Benue Trough: wrench-fault related basin on the border of the equatorial Atlantic. *Developments in Geotectonics. Elsevier*, pp. 787–819.
- Bosworth, W., Burke, K., 2005. Evolution of the red sea—Gulf of Aden Rift System. In: Post, P.J., Rosen, N.C., Olson, D.L., Palmes, S.L., Lyons, K.T., Newton, G.B. (Eds.), *Petroleum Systems of Divergent Continental Margin Basins*. SEPM Society for Sedimentary Geology, 0.
- Bosworth, W., Guiraud, R., Kessler, L., 1999. Late Cretaceous (ca. 84 Ma) compressive deformation of the stable platform of northeast Africa (Egypt): Far-field stress effects of the “Santonian event” and origin of the Syrian arc deformation belt. *Geology* 27 (7), 633–636.
- Brew, G., Litak, R., Barazangi, M., Sawaf, T., Zaza, T., 1999. Tectonic evolution of Northeast Syria: regional implications and hydrocarbon prospects. *GeoArabia* 4 (3), 289–318.
- Brew, G., Barazangi, M., Al-Maleh, K., Sawaf, T., 2001. Tectonic and geologic evolution of Syria. *GeoArabia* 6 (4).
- Bromhead, A., van Buchem, F.S.P., Simmons, M., Davies, R., 2022. Sequence stratigraphy, paleogeography, and petroleum plays of the Cenomanian-Turonian succession of the Arabian Plate. *J. Petrol. Geol.* 45 (2), 119–162.
- Capitanio, F.A., Morra, G., Goes, S., 2009. Dynamics of plate bending at the trench and slab-plate coupling. *Geochem. Geophys. Geosyst.* 10 (4).
- Chaimov, T.A., Barazangi, M., Al-Saad, D., Sawaf, T., Gebran, A., 1992. Mesozoic and Cenozoic deformation inferred from seismic stratigraphy in the southwestern intracontinental Palmyride fold-thrust belt, Syria. *Geol. Soc. Am. Bull.* 104 (6), 704–715.
- Core Lab, 1987. Azraq Basin Study. Unpublished report.
- De Ruiter, R., Lovelock, P., Nabulsi, N., 1995. The Euphrates Graben of eastern Syria: a new petroleum province in the northern Middle East. *Geo* 94, 357–368.
- Delaunay, A., Baby, G., Fedorik, J., Affifi, A.M., Tapponnier, P., Dymant, J., 2023. Structure and morphology of the Red Sea, from the mid-ocean ridge to the ocean-continent boundary. *Tectonophysics* 849, 229728.
- Diabat, A.A., 2007. Paleostress analysis of the Cretaceous-Tertiary rocks in central Jordan. *Dirasat Pure Sci.* 34 (2).
- Dilley, F.C., 1985. Cretaceous correlations in the Hamza wells nos. 1 to 5. *Paleontology Report No. 6*, NRA, Amman.
- Doutsos, T., Piper, G., Boronkay, K., Koukouvelas, I., 1993. Kinematics of the central hellenides. *Tectonics* 12, 936–953.
- Fallatah, M.I., Alnazghah, M., Kerans, C., Al-Hussaini, A., 2025. Geochemistry and regional stratigraphy of the Upper Cretaceous succession of central Saudi Arabia: a record of foreland basin inception on the Arabian Plate. *Cretac. Res.* 168, 106059.
- Farahpour, M.M., Hessami, K., 2012. Cretaceous sequence of deformation in the SE Zagros fold–thrust belt. *J. Geol. Soc.* 169 (6), 733–743.
- Farouk, S., Ahmad, F., Mousa, D., Simmons, M., 2016. Sequence stratigraphic context and organic geochemistry of Palaeogene oil shales, Jordan. *Mar. Petrol. Geol.* 77, 1297–1308.

- Freund, R., Garfunkel, Z., Zak, I., Goldberg, M., Weissbrod, T., Derin, B., 1970. The shear along the Dead Sea rift. *Phil. Trans. Roy. Soc. Lond.* 267, 107–130.
- Fritz, H., Abdelsalam, M., Ali, K., Bingen, B., Collins, A., Fowler, A., Ghebreab, W., Hauzenberger, C., Johnson, P., Kusky, T., 2013. Orogen styles in the East African orogen: a review of the neoproterozoic to cambrian tectonic evolution. *J. Afr. Earth Sci.* 86, 65–106.
- Garfunkel, Z., 1978. The Negev regional synthesis of sedimentary basins. In: *Sedimentology Guidebook, Pre-congress Excursion A: 10th International Congress on Sedimentology*, pp. 35–110. Jerusalem.
- Garfunkel, Z., 1981. Internal structure of the Dead Sea leaky transform (rift) in relation to plate kinematics. *Tectonophysics* 80 (1–4), 81–108.
- Glennie, K., Boeuf, M., Clarke, M.H., Moody-Stuart, M., Pilaar, W., Reinhardt, B., 1973. Late Cretaceous nappes in Oman Mountains and their geologic evolution. *AAPG Bulletin* 57 (1), 5–27.
- Guilmette, C., Smit, M.A., van Hinsbergen, D.J., Güre, D., Corfu, F., Charette, B., Maffione, M., Rabeau, O., Savard, D., 2018. Forced subduction initiation recorded in the sole and crust of the Semail Ophiolite of Oman. *Nat. Geosci.* 11 (9), 688–695.
- Guiraud, R., Bosworth, W., 1997. Senonian basin inversion and rejuvenation of rifting in Africa and Arabia: synthesis and implications to plate-scale tectonics. *Tectonophysics* 282, 39–82.
- Guiraud, R., Bosworth, W., Thierry, J., Delplanque, A., 2005. Phanerozoic geological evolution of Northern and Central Africa: an overview. *J. Afr. Earth Sci.* 43 (1–3), 83–143.
- Gvrtzman, G., Almogi-Labin, A., Moshkovitz, S., Lewy, Z., Honigstein, A., Reiss, Z., 1989. Upper Cretaceous high-resolution multiple stratigraphy, northern margin of the Arabian platform, central Israel. *Cretac. Res.* 10 (2), 107–135.
- Gvrtzman, Z., Garfunkel, Z., Gvrtzman, G., 1998. Birth and decay of an intracratonic magmatic swell: early Cretaceous tectonics of southern Israel. *Tectonics* 17 (3), 441–457.
- Hakimi, M.H., Abdullah, W.H., Alqudah, M., Makeen, Y.M., Mustapha, K.A., 2016a. Organic geochemical and petrographic characteristics of the oil shales in the Lajjun area, Central Jordan: origin of organic matter input and preservation conditions. *Fuel* 181, 34–45.
- Hakimi, M.H., Abdullah, W.H., Alqudah, M., Makeen, Y.M., Mustapha, K.A., 2016b. Reducing marine and warm climate conditions during the Late Cretaceous, and their influence on organic matter enrichment in the oil shale deposits of North Jordan. *Int. J. Coal Geol.* 165, 173–189.
- Hakimi, M.H., Abdullah, W.H., Alqudah, M., Makeen, Y.M., Mustapha, K.A., Hatem, B.A., 2018. Pyrolysis analyses and bulk kinetic models of the Late Cretaceous oil shales in Jordan and their implications for early mature sulphur-rich oil generation potential. *Mar. Petrol. Geol.* 91, 764–775.
- Hardy, C., Homberg, C., Eyal, Y., Barrier, É., Müller, C., 2010. Tectonic evolution of the southern Levant margin since Mesozoic. *Tectonophysics* 494 (3–4), 211–225.
- Homke, S., Vergés, J., Serra-Kiel, J., Bernaola, G., Sharp, I., Garcés, M., Montero-Verdú, I., Karpuz, R., Goodarzi, M.H., 2009. Late cretaceous–Paleocene formation of the proto–zagros foreland basin, Lurestan Province, SW Iran. *Geol. Soc. Am. Bull.* 121 (7–8), 963–978.
- Ibrahim, K.M., 1996. The Regional Geology of Al Azraq Area, Map Sheet No. 3553-I, Bulletin 36. Geology Directorate, Geological mapping Division, NRA, Amman.
- Ilani, S., Harlavan, Y., Tarawneh, K., Rabba, I., Weinberger, R., Ibrahim, K., Peltz, S., Steinitz, G., 2001. New K-Ar ages of basalts from the Harrat Ash Shaam volcanic field in Jordan: implications for the span and duration of the upper-mantle upwelling beneath the western Arabian plate. *Geology* 29 (2), 171–174.
- Joffe, S., Garfunkel, Z., 1987. Plate kinematics of the circum Red Sea—a re-evaluation. *Tectonophysics* 141 (1–3), 5–22.
- Johnson, C.A., Sattar, M.A., Rosell, R., Al-Shekailli, F., Al-Zaabi, N., Gombos, A., 2002. Structure and regional context of onshore fields in Abu Dhabi, UAE. In: *Abu Dhabi International Petroleum Exhibition and Conference. SPE. SPE-78488-MS*.
- Johnson, C., Hauge, T., Al-Menhali, S., Bin Sumaidaa, S., Sabin, B., West, B., 2005. Structural styles and tectonic evolution of onshore and offshore Abu Dhabi, UAE. In: *International Petroleum Technology Conference. IPTC. IPTC-10646-MS*.
- Jolivet, F., Faccenna, C., Agard, P., Frizon de Lamotte, D., Menant, A., Sternai, P., Guillocheau, F., 2016. Neo-Tethys geodynamics and mantle convection: from extension to compression in Africa and a conceptual model for obduction. *Can. J. Earth Sci.* 53 (11), 1190–1204.
- Karim, K.H., Koyi, H., Baziany, M.M., Hessami, K., 2011. Significance of angular unconformities between Cretaceous and Tertiary strata in the northwestern segment of the Zagros fold–thrust belt, Kurdistan Region, NE Iraq. *Geol. Mag.* 148 (5–6), 925–939.
- Kominz, M.A., Browning, J., Miller, K., Sugarman, P., Mizintseva, S., Scotese, C., 2008. Late Cretaceous to Miocene sea-level estimates from the New Jersey and Delaware coastal plain coreholes: an error analysis. *Basin Res.* 20 (2), 211–226.
- Kroonert, G., Affi, A.M., Al-Hajri, S.A., Droste, H.J., 2001. Paleozoic stratigraphy and hydrocarbon habitat of the Arabian Plate. *GeoArabia* 6 (3), 407–435.
- Kuss, J., 1992. The Aptian-Paleocene shelf carbonates of northeast Egypt and southern Jordan: establishment and break-up of carbonate platforms along the southern Tethyan shores. *Zeitschrift Deutsche Geologischen* 143, 107–132.
- Kuss, J., Bachmann, M., 1996. Cretaceous paleogeography of the Sinai Peninsula and neighbouring areas. *Comptes rendus de l'Académie des sciences. Série 2. Sciences de la terre et des planètes* 322 (11), 915–933.
- Lalami, H.R.K., Hajjalibeigi, H., Sherkati, S., Adabi, M.H., 2020. Tectonic evolution of the Zagros foreland basin since Early Cretaceous, SW Iran: regional tectonic implications from subsidence analysis. *J. Asian Earth Sci.* 204, 104550.
- Litak, R.K., Barazangi, M., Beauchamp, W., Seber, D., Brew, G., Sawaf, T., Al-Youssef, W., 1997. Mesozoic-Cenozoic evolution of the intraplate Euphrates fault system, Syria: implications for regional tectonics. *J. Geol. Soc.* 154 (4), 653–666.
- Litak, R.K., Barazangi, M., Brew, G., Sawaf, T., Al-Imam, A., Al-Youssef, W., 1998. Structure and evolution of the petroliferous Euphrates graben system, southeast Syria. *AAPG Bull.* 82 (6), 1173–1190.
- Lovelock, P., 1984. A review of the tectonics of the northern Middle East region. *Geol. Mag.* 121 (6), 577–587.
- Lüning, S., Kuss, J., Marlow, L., Kendall, C., Yose, L., 2014. Petroleum systems of the Tethyan region. In: *Marlow, L., Kendall, C., Yose, L. (Eds.), Petroleum Systems of the Tethyan Region*, 106. AAPG Memoir, pp. 217–239.
- Madanipour, S., Najafi, M., Nozaem, R., Vergés, J., Yassaghi, A., Heydari, I., Khodaparast, S., Soudmand, Z., Aghajari, L., 2024. The Arabia–Eurasia collision zone in Iran: tectonostratigraphic and structural synthesis. *J. Petrol. Geol.* 47 (2), 123–171.
- Makhlouf, I., Abu Azzam, H., Al-Hiayri, A., 1996. Surface and subsurface lithostratigraphic relationships of the cretaceous Ajlun group in Jordan, subsurface geology bulletin 8. Geology Directorate, Geological Mapping Division, Ministry of Energy and Mineral Resources, NRA, Amman.
- Marlow, L., Kendall, C.C.G., Yose, L.A., 2014. Petroleum Systems of the Tethyan Region, 106. AAPG Memoir, pp. 641–678.
- Mart, Y., Ryan, W.B., Lunina, O.V., 2005. Review of the tectonics of the Levant Rift system: the structural significance of oblique continental breakup. *Tectonophysics* 395 (3–4), 209–232.
- Masri, A., 2003. The geology of Dhiban (Wadi Al-Mujib), area map sheet No. 3152-1, 50k, bulletin 54. Geology Directorate, Geological Mapping Division, NRA, Amman.
- Masri, A., 2010. The geology of Batn Al Ghul (Jabal al Harad), area map sheet No. 3149-II, 50k, bulletin. *Geol. Dir. Geol. Mapp. Div.*, NRA, Amman 72.
- Matthews, K.J., Seton, M., Müller, R.D., 2012. A global-scale plate reorganization event at 105–100 Ma. *Earth Planet Sci. Lett.* 355, 283–298.
- McQuarrie, N., 2002. The kinematic history of the central Andean fold-thrust belt, Bolivia: implications for building a high plateau. *Geol. Soc. Am. Bull.* 114 (8), 950–963.
- Mehdawi, H.S., Mustafa, H.A., 2007. Petrography and geochemistry of the upper cretaceous-lower tertiary oil shale, NW-Jordan. *Basic Sci. & Eng.* 16 (2), 293–318.
- Meilijson, A., Ashkenazi-Polivoda, S., Ron-Yankovich, L., Illner, P., Alsenz, H., Spejger, R.P., Almogi-Labin, A., Feinstein, S., Berner, Z., Püttmann, W., 2014. Chronostratigraphy of the Upper Cretaceous high productivity sequence of the southern Tethys, Israel. *Cretac. Res.* 50, 187–213.
- Messaoud, J.H., Kalifi, A., Alibrahim, A., Ibrahim, K., Chirakal, T., Ardila Sanchez, M., Abu Leila, W., Ben Chabaane, N., Grélaud, C., Powell, J.H., van Buchem, F., 2025. Chronostratigraphy of the mixed Upper Cretaceous deposits at the northern margin of the Arabian Plate (Jordan). *Newsletters on Stratigraphy* 58 (2), 161–201. <https://doi.org/10.1127/nos/2025/0858>.
- Miall, A.D., 2013. *Principles of Sedimentary Basin Analysis*. Springer Science & Business Media.
- Miall, A.D., 2022. *Stratigraphy: the Modern Synthesis*, *Stratigraphy: A Modern Synthesis*. Springer, pp. 341–417.
- Mikbel, S., Zacher, W., 1986. Fold structures in northern Jordan. *Neus Jahrbuch für Geologie und Paläontologie Monatshefte* 4, 248–256.
- Miller, K.G., Kominz, M.A., Browning, J.V., Wright, J.D., Mountain, G.S., Katz, M.E., Sugarman, P.J., Cramer, B.S., Christie-Blick, N., Pekar, S.F., 2005. The Phanerozoic record of global sea-level change. *science* 310 (5752), 1293–1298.
- Mouthereau, F., Lacombe, O., Vergés, J., 2012. Building the Zagros collisional orogen: timing, strain distribution and the dynamics of Arabia/Eurasia plate convergence. *Tectonophysics* 532, 27–60.
- Mustafa, H., Atallah, M., Khuri, H., 1998. The upper cretaceous phosphate in NW-Jordan. *Pure. Sci. & Eng.* 7 (1), 73–114.
- Nairn, A., Alsharhan, A., 1997. *Sedimentary Basins and Petroleum Geology of the Middle East*. Elsevier.
- Najafi, M., Beamud, E., Ruh, J., Mouthereau, F., Tahmasbi, A., Bernaola, G., Yassaghi, A., Motamedi, H., Sherkati, S., Goodarzi, M.G.H., 2021. Pliocene growth of the Dowlatabad syncline in frontal arcs: folding propagation across the Zagros Fold Belt, Iran. *Bulletin* 133 (7–8), 1381–1403.
- Nichols, G., 2009. *Sedimentology and Stratigraphy*. John Wiley & Sons.
- Ninkabou, D., Agard, P., Nielsen, C., Smit, J., Haq, B., Rodriguez, M., Gorini, C., 2020. The Syn-And Post-obduction History of the Offshore North Oman Margin. *EGU General Assembly Conference Abstracts*, 22476.
- Papanikolaou, D., 2009. Timing of tectonic emplacement of the ophiolites and terrane paleogeography in the Hellenides. *Lithos* 108, 262–280.
- Piryaei, A., Reijmer, J., Borgomano, J., Van Buchem, F., 2011. Late Cretaceous tectonic and sedimentary evolution of the Bandar Abbas area, Fars region, southern Iran. *J. Petrol. Geol.* 34 (2), 157.
- Powell, J., 1989. Stratigraphy and sedimentation of the Phanerozoic rocks in central and south Jordan. *Bulletin. Geol. Dir. Nat. Resour. Authority (Ministry of Energy and Mineral Resources)*, Part B: Kurnub, Ajlun and Belqa Groups 11, 161, 12 figures, 17 tables., Amman.
- Powell, J.H., Moh'd, B.K., 2011. Evolution of Cretaceous to Eocene alluvial and carbonate platform sequences in central and south Jordan. *GeoArabia-Middle East Petrol. Geosci.* 16 (4), 29–82.
- Powell, J.H., Moh'd, B.K., 2012. Early diagenesis of Late Cretaceous chalk-chert-phosphorite hardgrounds in Jordan: implications for sedimentation on a Coniacian-Campanian pelagic ramp. *GeoArabia* 17, 17–38.
- Powell, J.H., Abed, A., Jarrar, G.H., 2015. Ediacaran Arabia complex of Jordan. *GeoArabia-Middle East Petrol. Geosci.* 20 (1), 99–156.
- Pufahl, P.K., Grimm, K.A., Abed, A.M., Sadaqah, R.M.Y., 2003. Upper Cretaceous (Campanian) phosphorites in Jordan: implications for the formation of a south Tethyan phosphorite giant. *Sediment. Geol.* 161 (3–4), 175–205.

- Quennell, A.M., 1958. The structural and geomorphic evolution of the Dead Sea Rift. *Q. J. Geol. Soc.* 114 (1–4), 1–24.
- Ricou, L.-E., 1971. Le croissant ophiolitique péri-arabe. Une ceinture de nappes mises en place au Crétacé supérieur. *Revue de géographie physique et de géologie dynamique* 13, 327–350.
- Ricou, L.-E., 1994. Tethys reconstructed: plates, continental fragments and their Boundaries since 260 Ma from Central America to South-eastern Asia. *Geodin. Acta* 7 (4), 169–218.
- Rioux, M., Garber, J., Bauer, A., Bowring, S., Searle, M., Kelemen, P., Hacker, B., 2016. Synchronous formation of the metamorphic sole and igneous crust of the Semail ophiolite: new constraints on the tectonic evolution during ophiolite formation from high-precision U–Pb zircon geochronology. *Earth Planet Sci. Lett.* 451, 185–195.
- Rioux, M., Garber, J.M., Searle, M., Crowley, J.L., Stevens, S., Schmitz, M., Kylander-Clark, A., Leal, K., Ambrose, T., Smye, A.J., 2023. The temporal evolution of subduction initiation in the Semail ophiolite: high-precision U–Pb zircon petrochronology of the metamorphic sole. *J. Metamorph. Geol.* 41 (6), 817–847.
- Schulze, F., Marzouk, A.M., Bassiouni, M.A., Kuss, J., 2004. The late Albian–Turonian carbonate platform succession of west-central Jordan: stratigraphy and crises. *Cretac. Res.* 25 (5), 709–737.
- Scotese, C.R., Vêrard, C., Burgener, L., Elling, R.P., Kocsis, A.T., 2025. The Cretaceous world: plate tectonics, palaeogeography and palaeoclimate. *Geol. Soc. London, Spec. Publ.* 544 (1). SP544-2024-28.
- Searle, M., 1985. Sequence of thrusting and origin of culminations in the northern and central Oman Mountains. *J. Struct. Geol.* 7 (2), 129–143.
- Searle, M., Rioux, M., Garber, J.M., 2022. One line on the map: a review of the geological history of the Semail Thrust, Oman-UAE mountains. *J. Struct. Geol.* 158, 104594.
- Segev, A., Sass, E., Schattner, U., 2018. Age and structure of the levant basin, Eastern Mediterranean. *Earth Sci. Rev.* 182, 233–250.
- Şengör, A.C., Stock, J., 2014. The Ayyubid Orogen: an ophiolite obduction-driven orogen in the late Cretaceous of the Neo-Tethyan south margin. *Geosci. Can.* 41 (2), 225–254.
- Shaw, J.E., Baker, J.A., Menzies, M.A., Thirlwall, M.F., Ibrahim, K.M., 2003. Petrogenesis of the largest intraplate volcanic field on the Arabian Plate (Jordan): a mixed lithosphere–asthenosphere source activated by lithospheric extension. *J. Petrol.* 44 (9), 1657–1679.
- Simmons, M.D., Bidgood, M.D., Davies, R.B., Droste, H., Levell, B., Razin, P., van Buchem, F.S., 2025. Intra-Turonian stratigraphic reorganization on the Arabian Plate. *Geol. Soc. London, Spec. Publ.* 545 (1). SP545-2023-207.
- Soudry, D., Glenn, C., Nathan, Y., Segal, I., VonderHaar, D., 2006. Evolution of Tethyan phosphogenesis along the northern edges of the Arabian–African shield during the Cretaceous–Eocene as deduced from temporal variations of Ca and Nd isotopes and rates of P accumulation. *Earth Sci. Rev.* 78 (1–2), 27–57.
- Stern, R.J., 1985. The Najd fault system, Saudi Arabia and Egypt: a late Precambrian rift-related transform system? *Tectonics* 4 (5), 497–511.
- Stern, R.J., Johnson, P., 2010. Continental lithosphere of the Arabian Plate: a geologic, petrologic, and geophysical synthesis. *Earth Sci. Rev.* 101 (1–2), 29–67.
- Stewart, S., 2016. Structural geology of the Rub' Al-Khali Basin, Saudi Arabia. *Tectonics* 35 (10), 2417–2438.
- Thuizat, R., Whitechurch, H., Montigny, R., Juteau, T., 1981. K–Ar dating of some infra-ophiolitic metamorphic soles from the Eastern Mediterranean: new evidence for oceanic thrustings before obduction. *Earth Planet Sci. Lett.* 52 (2), 302–310.
- Usman, M., Ardilla-Sanchez, M., Idiz, E., Abu-Mahfouz, I.S., van Buchem, F., Vahrenkamp, V., 2025. Organic and inorganic geochemical cyclicity of a Maastrichtian oceanic open-shelf carbonate source rock. *Nat. Sci. Rep.* 15, 15993. <https://doi.org/10.1038/s41598-025-99832-w>.
- Vaughan, A.P., Scarrow, J.H., 2003. Ophiolite obduction pulses as a proxy indicator of superplume events? *Earth Planet Sci. Lett.* 213 (3–4), 407–416.
- Veeken, P.C., 2006. Seismic Stratigraphy, Basin Analysis and Reservoir Characterisation, 37. Elsevier.
- Vergés, J., Casini, G., Ruh, J., Cosgrove, J., Sherkat, S., Najafi, M., Casciello, E., Saura, E., Fard, I.A., Piryaee, A., 2024. Structural style and timing OF NW-SE trending zagros folds IN SW Iran: interaction with north-south trending arabian folds and implications for petroleum geology. *J. Petrol. Geol.* 47 (1), 3–73.
- Vicente de Gouveia, S., Besse, J., Frizon de Lamotte, D., Greff-Leffitz, M., Lescanne, M., Gueydan, F., Leparmentier, F., 2018. Evidence of hotspot paths below Arabia and the Horn of Africa and consequences on the Red Sea opening. *Earth Planet Sci. Lett.* 487, 210–220.
- Vincent, B., van Buchem, F.S., Bulot, L.G., Jalali, M., Swennen, R., Hosseini, A., Baghban, D., 2015. Depositional sequences, diagenesis and structural control of the Albian to Turonian carbonate platform systems in coastal Fars (SW Iran). *Mar. Petrol. Geol.* 63, 46–67.
- Wald, R., Segev, A., Ben-Avraham, Z., Schattner, U., 2019. Structural expression of a fading rift front: a case study from the Oligo-Miocene Irbid rift of northwest Arabia. *Solid Earth* 10 (1), 225–250.
- Walley, C.D., 1998. Some outstanding issues in the geology of Lebanon and their importance in the tectonic evolution of the Levantine region. *Tectonophysics* 298 (1–3), 37–62.
- Watts, A.B., 2001. *Isostasy and Flexure of the Lithosphere*. Cambridge University Press.
- Ye, J., Afifi, A., Rowaihy, F., Baby, G., De Santiago, A., Tasianas, A., Hamieh, A., Khodayeva, A., Al-Juaied, M., Meckel, T.A., 2023. Evaluation of geological CO₂ storage potential in Saudi Arabian sedimentary basins. *Earth Sci. Rev.* 244, 104539.
- Ziegler, M.A., 2001. Late Permian to Holocene paleofacies evolution of the Arabian Plate and its hydrocarbon occurrences. *GeoArabia* 6 (3), 445–504.